T6SS in *Pseudomonas aeruginosa*: A novel model for toxin delivery

Jacqueline Corbitt

A dissertation
submitted in partial fulfillment of the
requirements for the degree of

Doctor of Philosophy

University of Washington

2017

Reading Committee:

Paul Wiggins, Chair

Jens Gundlach

Marcel den Nijs

Program Authorized to Offer Degree:
Physics

University of Washington

Abstract

T6SS in *Pseudomonas aeruginosa*: A novel model for toxin delivery

Jacqueline Corbitt

Chair of the Supervisory Committee:
Professor Paul Wiggins
Physics & Bioengineering

The Type Six Secretion System (T6SS) is a bacterial toxin-delivery system targeting bacterial cells which neighbor the donor, promoting recipient cell death. The T6SS is widely conserved among Gram-negative bacteria and may be a central determinant in bacterial fitness in polymicrobial communities of particular relevance to chronic infection. Sequence homology of secretion system components to the T4 bacteriophage tail spike, cryoEM reconstructions of the secretion system and fluorescence imaging are all consistent with a dynamic mechanism of secretion. The complex system, which is composed of at least 15 proteins, forms a puncturing apparatus/delivery system which uses a donor protein filament to puncture the recipient cell wall to deliver protein toxins. Using quantitative imaging analysis of multiple fluorescent fusions, we present a detailed characterization of T6SS system dynamics visualized in single cells in multiple bacterial species, developing a model of T6SS function. We present quantitative measurements of the dynamics of the secretion system - from the assembly to contraction to disassembly - in conjunction with quantitative measures of system function, including recipient cell lysis.

TABLE OF CONTENTS

Page

LIST OF FIGURES

Figure Number Page

ACKNOWLEDGMENTS

My mother, Karen Corbitt, inspired my love of science from a young age through her personal example and interest. Her own achievements and consistent support showed me that I could set lofty goals and could achieve them through hard work. My father was a great example of patience and determination, and showed consistent love to his entire family. On my hardest days, I reminded myself that I was their daughter and that meant I could do anything. I am grateful for the support of my siblings, Kyle, Christina, Scott, and David Corbitt, who never once doubted my academic dreams and were consistently both willing to be a listening ear and kept me laughing through the good and the hard days. Alex Swan has been with me for half of my graduate career, and his constant encouragement and faith in me kept me buoyed and committed to reaching this goal.

My high school physics teacher, Thomas Haff, nurtured the love for physics that I brought to class and to this day encourages me to continue pursue greater skill in the field. I want to recognize my high school calculus teacher, Ms. Crain (now Mrs. Baxter), for the toughest class I had experienced at that point at a crucial moment in my life. Developing my identity both as a mathematician and as someone who can take on overwhelming challenges has shaped my character for all the years since. I also want to thank Ms. Dean for offering the most difficult English class I have had in my entire academic career, preparing me for the writing challenges faced in both schoolwork and academic papers.

I want to thank Dr. Gus Hart at Brigham Young University for offering me the chance to be part of his lab my first month in university, providing me with invaluable research experience, writing and speaking skills, and the confidence boost to be explicitly invited

to join a research group so early in my career. I want to thank Dr. Steve Turley and Dr. David Allred for being fantastic mentors and great examples of both character and physicists.

The Wiggins lab has been a wonderful place to work. Julie Cass, Sarah Mangiameli, and Colin LaMont have been exceptional lab mates, always willing to help both inside and outside the lab. I want to particularly recognize Stella Stylianidou, who was my roommate for two years before we joined the same lab and has thus been an integral part of my graduate school experience, going through the ups and downs together. Additionally, the undergraduates I worked with, Brandon Hoang, Ian Davis, and Jun Seok Yeo were inspirations to me in their willingness to take on new material and learn both programming and biological techniques. I worked with each of them for a year, and their work is invaluable in both main chapters of my thesis.

This work would not be possible without collaboration with the Mougous lab. Michele LeRoux, Robin Kirkpatrick, and S. Brook Peterson were all invaluable in creating strains, thinking of new experiments, and providing feedback. Joseph Mougous has improved my understanding of microbiology and helped develop my intuition in many scientific aspects.

I would like to thank my committee members, Jens Gundlach, Marcel den Nijs, Subhadeep Gupta, Sarah Keller, and Joshua Vaughan. I would specifically like to thank the members of my reading committee, Jens Gundlach and Marcel den Nijs, as well as Joshua Vaughan for going above and beyond his role as mentor on my committee.

Finally, thanks to my graduate advisor, Paul Wiggins. He has been an exceptional advisor throughout my graduate career, with consistent enthusiasm and positivity, dedication to his discipline, and a constant willingness to explain any topic in thorough detail. I am fortunate to have had the opportunity to train in his lab.

DEDICATION

to my family and friends, for their constant support

Chapter 1

INTRODUCTION

1.1 Bacterial Secretion Systems

1.1.1 Types of Bacterial Secretion Systems

Bacterial secretion systems are widespread among bacterial species. They serve to deliver proteins, enzymes, or toxins from the interior of the bacterial cell to the exterior, playing a role in responsiveness to the external environment as well as adhesion, pathogenicity, adaptation, and survival [17]. To facilitate these roles, many secretion system types have developed; in fact, Gram-negative bacteria alone utilize seven types of secretion systems, indicating that secretion systems promote bacterial fitness. Indeed, only one clade of diderm (having two cell walls) bacteria, *Thermotogae*, lacks any type of known secretion system [2].

The high number of secretion system types suggests there is structural variance between secretion mechanisms. Understanding secretion mechanisms and their responses to outside stimuli is fundamentally important to understanding interbacterial interactions. Several types of secretion systems (T3SS, T4SS, T6SS) have been shown to have antibacterial behavior, frequently directly targeting neighboring bacteria. In these cases where secretion systems target surrounding bacteria, rapidly acting secretion systems are at an advantage when target molecules or bacteria are planktonic or otherwise moving rapidly. One example of a quick acting secretion system is the T6SS in *V. cholerae*, which forcibly fires toxic effectors into a neighboring bacterium in less than a second and then promptly disassembles [6]. This single shot delivery mechanism does not require target bacteria to remain at rest, but rather delivers a load of effectors in one shot before

the apparatus is disassembled and recycled elsewhere. In contrast, slowly acting secretion systems require more stationary surroundings, such as in cases where secretion acts to gather nutrients from the environment or delivers toxins to neighboring bacteria in a biofilm. For instance, RND pumps depend on a two-step mechanism driven by a proton gradient, which inherently limits the speed of delivery [17]. This slower mechanism is used primarily for general antibacterial compounds, and its purpose is independent of contact with neighboring bacteria [17]. In short, each mechanism and its corresponding rate of action are optimized to the function it performs. Therefore, studying mechanism can also help researchers understand secretion system function.

Studying the secretion mechanism in tandem with the method of activation of the secretion system also lends to a better understanding of the secretion system purpose. Surprisingly, despite holding key roles in many cell processes, none of the known secretion systems is constitutively active in any species [17]. Thus, each new secretion system must be analyzed to uncover the conditions under which the secretion system is activated. One proposed activation mechanism for contact-dependent secretion systems is the recognition of host receptor by adhesins [23]. This possible contact-dependent activation mechanism could lend itself to tit-for-tat targeting in *V. cholerae* T6SS, as described in [8]. Activation of some other secretion systems relies on contact with other cells, such as T3SS [33]. T3SS, T4SS, and T6SS are all secretion systems designed to inhibit growth of other bacterial species. It seems likely that these systems may have developed a contact-dependent activation mechanism to both sense neighboring bacteria and signal creation of the tools to attack them with [17].

1.1.2 Roles of Bacterial Secretion Systems in Multi-species Bacterial Communities

Bacterial pathogens secrete molecules to influence their surrounding environment, protect themselves and gain nutrients to maximize their evolutionary success. Within communities containing multiple species of bacteria, even slight competitive advantages over

neighbors can yield large effects over time in both relative quantities of the species as well as the health of the host organism [68]. This advantage can lead to to catastrophic consequences; in particular, the secretion systems T3SS, T4SS, and T6SS contribute to the virulence of many Gram-negative bacteria known for causing dangerous and sometimes deadly infections in patients worldwide [54]. Given that many model bacterial species, including *V. cholerae*, *B. thailandensis*, *P. aeruginosa*, and *E. coli*, divide every 30-40 minutes under normal lab conditions, a simple calculation suggests that even a 1% growth advantage over another species of bacteria can result in an order of magnitude difference in population in a few hours (for example, over five hours, roughly 10 doubling events occur: $1.01^{10} = 1.10$). Contact-dependent cell killing provides one of those small advantages. Contact-dependent cell killing mechanisms rely on several factors which depend on several events concomitantly. For instance, each firing cell must accurately aim and deliver a sufficient amount of toxins to a neighbor cell which must be of a different species and susceptible to the particular toxins delivered. Unsurprisingly, the combination of all factors needed to achieve efficient cell killing is not always achieved, as shown in Δ*retS P. aeruginosa*, a background in which H1-T6SS is constitutively active and where even effective targeting of cells of different susceptible species does not immediately result in cell death, but small advantages over generations quickly add up under the exponential growth conditions of bacteria [40].

These small advantageous factors manifest themselves in other ways beyond cell killing. For example, T6SS has been shown to play a role in biofilm formation in *E. coli*, possibly through eliminating nearby bacterial competitors over multiple bacterial lifecycles [3]. In this and other consequences of T6SS activity, T6SS is not shown to be the primary factor in determining pathogenicity, but rather contributes over time to growth of *E. coli*, allowing it the nutrients and space to create a biofilm [9].

In T6SS in *P. aeruginosa*, effectors target the cell wall peptidoglycan, the inner and outer membrane, and nucleic acids (as well as possibly other unknown cytoplasmic targets) [57]. These targets are conserved and essential components of bacteria, allowing the T6SS

to be a versatile attacker against virtually all bacterial species. Interestingly, peptidoglycan, against which several of the *P. aeruginosa* H1-T6SS effectors act, is not a component of eukaryotic cell walls, suggesting that the H1-T6SS is designed specifically for antibacterial purposes, although the effectors can have antieukaryotic behavior as well by acting against phospholipids [57].

1.1.3 H1-T6SS in P. aeruginosa

The T6SS is a multisubunit protein complex (around 13-15 proteins, depending on the species and often on system regulation) which may have either or both anti-prokaryotic and anti-eukaryotic cell properties. Discovered in 2006 in the Mekalanos lab [46], this system has been shown to deliver toxic effectors between cells. The systems are commonly found in Gram-negative bacteria ($\approx 25\%$ of all Gram-negative bacteria studied have at least one copy of the T6SS) and have a range of enzymatic activities [57]. Each T6SS toxin is paired with an immunity protein to prevent damage to the donor cell from itself and from kin cells [30, 56]. While structural homology in some systems, including *V. cholerae*, closely resembles contractile bacteriophage, the mechanism of delivery has not been well-studied in other species containing T6SS. This is possibly due to the breadth and depth of investigation into the mechanism of *V. cholerae*, which closely resembles both structurally and functionally the bacteriophage delivery mechanism; since the proteins in T6SS bear close genetic relation to the bacteriophage proteins, this connection is plausible and has not been investigated in much detail in species outside *V. cholerae*.

This thesis focuses particularly on the role of the Hcp-secretion-island 1 Type VI Secretion System (H1-T6SS) in *Pseudomonas aeruginosa*. *P. aeruginosa* is a Gram-negative opportunistic pathogen involved in many clinically problematic infections, such as lung infection in cystic fibrosis patients and chronic or acute infections in hospitals. One of the primary reasons that *P. aeruginosa* is so effective under these conditions is its ability to attack surrounding bacteria, diminishing competition for resources. This ability stems in

great part from its three copies of T6SS (labeled H1- to H3-T6SS), which act independently from each other and deliver distinct effectors which have a range of consequences in the recipient cells. Some of the noted differences in the copies of T6SS have to do with the chosen targets; H1-T6SS only targets prokaryotic cells, while H2- and H3-T6SS inject at least three different toxins associated with epithelial cells, suggesting that these secretion systems target both prokaryotic and eukaryotic cells. Overall, these T6SSs help *P. aeruginosa* outcompete other bacteria under several clinically relevant conditions, and are important in understanding the consequence of infection in the host organisms.

1.1.4 Common Mechanisms of Secretion

Known secretion mechanisms consist of proteins which span one or both cell membranes, creating a pore for substrates to pass through. The delivery mechanisms are sometimes passive, as in the case of RND pumps which use proton gradients, but are often active, powered by ATP hydrolysis (T1SS) or rotary motion (T2SS) [17]. Passive mechanisms, such as RND pumps and the T1SS, are used to transport a variety of molecules across the cell envelope, anything from ions to drugs to proteins. These substrates, often not critically time-dependent, provide a passive mechanism well-suited for for substrate delivery. In contrast, active mechanisms can be timed to quickly respond to environmental cues. In the case of T3SS, T4SS, and T6SS, all of which have more active secretion mechanisms, effector proteins are delivered directly to a neighboring cell, and so timing becomes more crucial in effective delivery.

One well-studied active mechanism is the T6SS in *V. cholerae*. Much of this study has been done in particular by the Mekalanos and Basler labs. Several proteins in T6SS are conserved between species, in particular TssB, TssC, and ClpV [12]. In Basler and Mekalanos' 2012 paper, they showed images of TssB-GFP structures extending across the width of the cell, which then contracted to approximately half their length on the order of milliseconds (Fig. 1.1) [7]. This structure, also observed through electron crytomography,

appeared to be roughly perpendicular to the cell wall, maximizing delivery efficiency (Fig. 1.2). Mekalanos and Basler theorize that the contraction of this sheath pushes the T6SS spike and inner tube complex out of the donor cell and into a target cell [7]. Disassembly of this contracted sheath depends on ClpV, an AAA+ adenosine triphosphatase (ATPase) that complexes with the TssBC sheath in vivo and disassembles these structures [10, 51]. Basler *et al.* showed that in *V. cholerae*, ClpV associates with the contracted TssBC sheath on average within a second of contraction [6]. Using amino acid mutations, Bonemann and Pietrosiuk *et al.* demonstrated that the N-terminal domain of ClpV binds to the N terminus of TssC in vivo, and, combined with the fact that ClpV only binds to the TssBC sheath after contraction, which seems to conclude that the binding site on TssC is only exposed to ClpV after the sheath contracts [6, 10, 51]. Altogether, this builds a model suggesting that in *V. cholerae*, TssBC builds a sheath which spontaneously contracts, pushing the VgrG spike, the inner tube, and effectors into the neighboring cell. After effector delivery into the neighboring cell, the sheath is disassembled by ClpV, freeing the components to be reused to create another T6SS apparatus. See Fig. 2.1. While this apparatus is well-characterized in *V. cholerae*, interestingly no study currently published has addressed whether the same mechanism holds true in other bacterial species.

1.2 Bacterial Sensing of Environment

Several systems play a role in bacterial sensing of the environment. In addition to chemotaxis, bacteria utilize a cytosolic receptor-transducer, or a transmembrane histidine kinase connected with a response regulator, or with a receptor associated to the histidine kinase to sense their surroundings [18, 73, 52, 21]. One-component systems typically sense stimuli in the cytosol and respond correspondingly, while two-component stimuli respond to external stimuli, including nutrients, redox state, osmolarity changes, quorum signalling, antibiotics, temperature, chemoattractants, and pH [28]. Each of these stimulants could prompt secretion mechanisms to activate.

Several secretion mechanisms, in addition to sensing nutrients and small molecules,

might sensibly be prompted by sensing neighboring bacteria. In particular, T3SS, T4SS and T6SS are all contact-dependent inhibition mechanisms of neighboring bacteria; in these cases, it could be particularly important for these secretion mechanisms to sense threats from surrounding bacteria and either activate secretion or direct secretion toward a bacterial target. Earlier, adhesins were mentioned as one possible mechanism of neighbor sensing [23]. Another sensing mechanism, quorum sensing interestingly appears to inhibit both the H1-T6SS in *P. aeruginosa* as well as the *vas* system of *V. cholerae* O1 strains, suggesting that these systems are more active under low cell density conditions and may work to effectively displace competing bacteria from the surrounding area, promoting resources for growth of its own colonies [34, 42, 57]. In contrast, H2-T6SS in *P. aeruginosa* is induced under conditions of high cell density, suggesting this system is most effective when an established colony of *P. aeruginosa* needs to protect itself from invading species [57]. Possibly related to quorum sensing, LeRoux *et al.* has suggested that *P. aeruginosa* senses sister cell lysate and responds through activation of Hcp secretion island I encoded T6SSS (H1-T6SS) [41].

1.3 T6SS regulation

The *Vibrio*, *Burkholderia*, and *Pseudomonas* species tend to have T6SS gene clusters throughout several members of their species. Activation of T6SS has been studied in many of these species, and T6SS activation in some of the more studied and prevalent species is discussed below.

1.3.1 Vibrio species

Most *Vibrio* T6SS investigation has centered around *V. cholerae*, the aetiological agent of cholera. This genus has more than 200 serogroups, but the majority of *V. cholerae* strains hold the entire complement of T6SS genes, indicating that T6SS is critical in the *V. cholerae* lifestyle and interbacterial interactions [45].

Strains of *V. cholerae* differ dramatically in T6SS regulation and sensitivity [45]. External conditions such as salinity and quorum sensing all play different roles in activating T6SS in the various *V. cholerae* strains. For instance, the *V. cholerae* strains A1552, E7946 and 93Ag49 are more active and produce and secrete Hcp under high salinity conditions, in contrast to standard laboratory conditions where Hcp is produced but not secreted [45]. Additionally, increased killing of *Escherichia coli* MC4100 by the *V. cholerae* strain A1552 is observed under high salt concentration conditions [45]. This observation is sensible given that *V. cholerae* naturally occurs in the ocean or in brackish waters, places of high salt concentration [45]. In strain C6706, quorum sensing is mediated via environmental autoinducer concentration; at low cell density, the response regulator LuxO is phosphorylated and induces the transcription of small quorum-regulatory RNAs, which bind and destabilize the master regulator HapR [45]. The master regulator can repress virulence genes but also activate expression of important *V. cholerae* T6SS proteins such as HapA, thus having both positive and negative effects on T6SS gene expression [45]. In some other strains, such as A1552, AJ3 and AJ5 (but not C6706) T6SS genes are upregulated at high cell density (in contrast to being downregulated at low cell density) [45].

While of the *Vibrio* family T6SS has been most closely studied in *V. cholerae*, quorum sensing also plays a vital role in T6SS activation in other *Vibrio* species. Quorum sensing is crucial for *hcp* expression in *Vibrio parahaemolyticus*, but has opposing effects on two distinct T6SS gene clusters, indicating that likely one system is active at high-cell density and another at low-cell density [45]. In *Vibrio alginolyticus*, two T6SS gene clusters are present, yet only one is regulated through quorum sensing [45]. Results indicate that in this species, T6SS is actually upregulated under low cell density conditions, likely indicating that different mechanisms are more effective at cell killing under different conditions [45].

1.3.2 Burkholderia species

The *Burkholderia* genus includes *Burkholderia mallei* (Glanders disease), *Burkholderia pseudomallei* (melioidosis), *Burkholderia cepacia* (human lung infections), and *Burkholderia thailandensis* (rarely infects humans or animals). *B. mallei* and *B. thailandensis* possess five T6SS clusters and *B. pseudomallei* possesses six [59]. One species possessing multiple T6SS gene clusters indicates that strict regulation over each cluster is required, as well as suggests that each T6SS has unique targets. In line with this hypothesis, T6SS-5 in *B. thailandensis* targets eukaryotes, while T6SS-1 targets prokaryotes [61]. Regulation of T6SS in several important *Burkholderia* species is discussed below.

The T6SS-1 gene cluster in *Burkholderia mallei* and *Burkholderia pseudomallei* is carefully regulated, depending strongly on overexpression of VirAG TCS or uptake by phagocytic cells [13, 45]. *B. pseudomallei*) specifically is a Gram-negative bacterial pathogen with copies of both T3SS and T6SS [13]. In this species, T3SS-3 and T6SS-1 have been shown to be involved in bacterial virulence in mammals. Chen *et al.* showed that the same pathway activated both T3SS-3 and T6SS-1 in these species; however, the method of activation depended on the environmental conditions [13]. In medium, T6SS-1 gene expression was fully dependent on BprC, but in mammalian host cells, expression depended on a two-component sensor-regulator [13]. These two different activation stimuli use alternative transcriptional start sites and clearly show the dependency of activation on specific external conditions [13]. This surprising result likely indicates that these systems work in conjunction in virulence in mouse infection [45].

AtsR is a negative response regulator of T6SS genes in *B. cenocepacia* [4]. It bears many similarities to RetS in *P. aeruginosa*; inactivation of AtsR in *B. cenocepacia* increases biofilm formation and hypersection of Hcp [4].

B. thailandensis is of particular relevance for this study, as we use it as a T6SS competitor for *P. aeruginosa* as described in 1.3.3. This species has a constitutively active T6SS under laboratory conditions, and as mentioned earlier is not commonly implicated in in-

fections in either humans or animals, making it an ideal choice for study.

1.3.3 Pseudomonas species

Pseudomonas species are widespread and diverse, with nearly 200 characterized species [19]. These species thrive in a variety of conditions, including soil, water, and host organisms, and thus are very adaptable [49]. 90 *Pseudomonas* strains have genomic information on file, and analysis of 34 of these strains indicates 70 T6SSs with at least one T6SS gene cluster per strain, with the exception solely of *Pseudomonas stutzeri* A1501 [63, 5]. Plant pathogens, including *Pseudomonas syringae*, contain T6SS gene clusters as well as another pathogenic secretion system, T3SS [1, 48, 55]. In contrast, *P. aeruginosa* contains several varieties of secretion systems, and three evolutionarily distinct T6SSs [46]. H1-T6SS is discussed in more detail below (see 1.3.3). H2- and H3-T6SSs are crucial for pathogenesis against *Arabidopsis thaliana*, a flowering plant often used as a model organism in plant biology [42]. Interestingly, H2-T6SS deletion weakens the concentration of *P. aeruginosa* bacteria in mouse infection and H3-T6SS is upregulated when exposed to epithelial cell extracts [14, 42, 66]. Together these indicate that the various T6SS gene clusters in *P. aeruginosa* are most effective against very different targets, ranging from bacteria to plants to mammals. This at least in part explains the reason behind multiple copies of T6SS. With regards to T6SS activation, H1-T6SS and H3-T6SS are differentially regulated during biofilm development, implicating differing responses to quorum sensing [65]. This suggests that strict regulation of T6SS gene expression is key for an optimized virulence mechanism [9, 42, 46].

Other *Pseudomonas* species are regulated by similar proteins as H1-T6SS, although the activation pathway may differ between species. For instance, RetS and LadS antagonistically regulate T6SS in *Pseudomonas syringae*, but in contrast to RetS in *P. aeruginosa*, the RetS and LadS seems to be parallel to (not upstream of) the GacS/GacA TCS [55]. Again similar to the regulation of H1-T6SS in *P. aeruginosa*, in *Pseudomonas fluorescens* Pf-5 and

Pseudomonas brassicacearum the GacS/GacA two component regulatory system regulate the expression of T6SS genes, as deletion of either of these proteins diminishes T6SS gene expression compared with wild type [26, 38].

To round out current knowledge about T6SS activation for the *Pseudomonas* species, *Pseuodomonas entomophila* and *Pseudomonas mendocina* are both used as bacterial models for characterizing mechanisms of regulation *in silico* [58].

H1-T6SS P. aeruginosa activation

One of the best characterized T6SSs is the H1-T6SS in *P. aeruginosa*. H1-T6SS is critical in chronic infections, demonstrated in the rat model of chronic respiratory infection and in chronically infected cystic fibrosis patients [46, 53]. Unlike the *V. cholerae* T6SS which is constitutively active, the *P. aeruginosa* H1-T6SS appears to be highly regulated [6]. Although three activation pathways for the H1-T6SS have been discovered to date, little is known about how these regulatory pathways affect T6SS dynamics and function. One activation pathway is post-translational regulation by the threonine phosphorylation pathway (TPP). In this pathway, a fork head-associated domain (FHA) protein, Fha, is phosphorylated by kinase PpkA which precipitates T6SS assembly and effector secretion [47]. A phosphatase, PppA, counteracts the phosphorylation of Fha, restoring the system to its inactive state. Two impetuses are thought to activate the TPP: surface-associated growth and membrane perturbation [8, 64].

A more recently characterized activation method is the *P. aeruginosa* response to antagonism (PARA) (e.g. [41]) in which H1-T6SS is activated in *P. aeruginosa* when the cell is exposed to *P. aeruginosa* cell lysate. Although efficient T6SS effector delivery is contact-dependent, its activation by PARA appears to be contact-independent. LeRoux *et al.* also demonstrated that PARA activation is independent of TPP, and instead works through the global activation of antibiotic and cyanide synthesis/regulator of secondary metabolism (Gac/Rsm) pathway.

The Gac/Rsm pathway is a global regulatory system which affects production of proteins through RsmA, a CsrA-type protein which predominantly represses translation of target mRNA molecules to which it binds [39]. PARA also occurs together with changes in T6SS gene expression, further indicative that this pathway is separate from the TPP, a post-translational regulator of H1-T6SS [41]. Protein regulators of this system include RetS, LadS, and GacS, which regulate both H1-T6SS and T3SS during acute and chronic *P. aeruginosa* infections [16, 71]. RetS and LadS are noncoupled hybrid sensor kinases that counteract each other. RetS downregulates biofilm formation and T6SS gene expression, but upregulates T3SS; LadS does the opposite [71, 70, 11]. Additionally, both H1-T6SS and T3SS are regulated in part by the GacS/GacA two component signaling system. Phosphorylation of GacA increases transcription of sRNAs *rsmZ* and *rsmY*, which result in opposite regulation of the T3SS and H1-T6SS. As mentioned earlier, these Gac proteins are also relevant in *Pseudomonas syringae*, *Pseudomonas fluorescens* Pf-5, and *Pseudomonas brassicacearum*.

The last known activation pathway, TagF, is less well understood. TagF is a post-translational repressor of the H1-T6SS and is present in several T6SSs which lack Fha and PpkA [12, 64]. Additionally, it shares homology with the actin regulatory profilin, including the surface used by profilin to bind poly-proline sequences [64]. Interestingly, Fha contains a proline-rich domain which is phosphorylated by PpkA, although TagF activation is independent of p-Fha [47, 64]. Based on these observations, Silverman *et al.* hypothesized that TagF interacted with pppA [64]. However, a recent IP/MS of Fha and its potential partners indicates that TagF does not directly bind to Fha (Mougous lab, unpublished). TagF deletion is shown to activate H1-T6SS independent of TPP and PARA [41].

As a note, the rates of H1-T6SS activation are not equal for each of these activation methods. Δ*retS* has the highest H1-T6SS activity rate of any of the activation methods described in this section: ≈20% of all *P. aeruginosa* cells have at least one H1-T6SS focus over a 9 minute timelapse. In contrast, cells activated via PARA, Δ*pppA*, or Δ*tagF* have

close to half that activity over the same time frame.

Although many of the components of these three activation pathways have been thoroughly investigated, little is yet understood quantitatively about the either the wild-type or mutant dynamics of H1-T6SS and how the dynamics is influenced by neighbor-cell contact of either same-species or competitor-species bacteria. Due to the stochastic nature of the secretion-system assembly and disassembly both at subcellular positions with and without cell contact, a quantitative analysis will play a central role in understanding how activity is regulated.

1.4 P. aeruginosa H1-T6SS targeting

An important question in secretion system study, particularly for secretion systems with antibacterial activity on the cell level, is whether the cell can target its machinery directly at competitor cells. There are in the literature currently two primary methods of measuring targeting, shown in Fig. 1.3. Panel A shows fluorescence microscopy observations, where T6SS foci can be shown to line up across from each other, and Panel B shows 7-hour competitions which measure T6SS killing between species.

Foci matching (Fig. 1.3 Panel A) has been studied in the Δ*retS* and the Δ*pppA* strains, with clear foci matching in Δ*retS* and negligible foci matching in Δ*pppA*. The latter observation can be explained by recalling that by deleting *pppA*, Fha H1-T6SS foci formed through the TPP pathway cannot be deactivated and are therefore permanently in the same location within the cell. Surprisingly, although foci matching does appear to occur by eye in the Δ*retS* background, no current publications compare the observed foci matching to random, so it is not immediately clear whether the observed foci matching is significant or not.

Competitions such as the one in Fig.1.3 Panel B have frequently been applied to demonstrate that *P. aeruginosa* T6SS killing is selective between recipients with a secretion system and those without across all mentioned activation methods [8, 40, 41]. This competition data has been used to bolster the idea that *P. aeruginosa* H1-T6SS must be foci-matching

in all deletions. However, all experiments (except in one case in the Δ*retS* background) mixed the *P. aeruginosa* strain with either a secretion system positive or secretion system negative competitor, but not both. The prominent killing of secretion system positive recipient bacterial species can be explained via PARA; the secretion system positive recipients lysed a sufficient number of *P. aeruginosa* cells to activate the *P. aeruginosa* H1-T6SS above average, whereas the secretion system negative recipients caused no lysis and therefore there was no *P. aeruginosa* H1-T6SS activation. PARA activation was discovered after many of the T6SS competition studies in *P. aeruginosa* were published, so this confounding factor was not accounted for in the competitions. The exception is in one experiment in the Δ*retS* background, where Δ*retS P. aeruginosa* was able to distinguish between T6SS+ and T6SS- competitors and preferentially killed the T6SS+ competitors [8].

Given the above data, Basler *et al.* has proposed a model where *P. aeruginosa* can sense its environment via membrane perturbations and correspondingly activate H1-T6SS at the location of membrane perturbation [8].

1.5 Microscopy

The work done in this thesis uses both phase-contrast microscopy and fluorescence microscopy to respectively identify individual cells and to track essential T6SS proteins. Cells are grown in Luria broth (LB) then mounted on an gel (composed of minimal media, nitrate, and 2% agar) kept in place by a rubber gasket on a transparent glass slide. Upon being placed on the slide, cells enter lag phase for up to 30 minutes, but then begin log phase; the slide's gel provides sufficient nutrients to support several hours of cell division. The following sections describe the process of visualization of T6SS proteins in single-cell, real-time analysis.

1.5.1 Phase contrast microscopy

Bacterial cells are almost transparent when viewed with a simple bright field microscope. However, incident light experiences a phase shift when passing through a specimen. Phase shifts are most often invisible to the human eye, since photographic equipment and the human eye are only attuned to the amplitude changes of light. Thus, transforming phase changes into amplitude differences of light is imperative to identifying small, nearly transparent objects. It is this phenomenon which is exploited in phase contrast microscopy.

The fundamental principle behind making phase changes visible is to isolate the background incident light from the light scattered by the sample. This is performed by both creating destructive interference between scattered and unaffected incident light and by limiting the amount of unaffected incident light in the image plane. This results in a relative diminished amplitude of light which has been scattered by the sample, and creates a dark image of the specimen with a bright background.

It is important to note here that this technique yields a clear image of the cell but not its inner workings. See Fig. 2.9 Panel A. The method of visualizing inner proteins of the cell is described in the next section.

1.5.2 Fluorescence microscopy

Observing inner workings of the cell at an individual level in real-time is imperative to thoroughly understand cell and process function. Fluorescence microscopy is a well-established technique which allows investigators to observe both localization and dynamics of proteins of interest at a subcellular level in real time. The essential principle is the absorption and re-radiation of light by protein fluorophores which are genetically attached to the protein of interest. The light emitted from the fluorophore can then be used to track the protein of interest. The time between exciting the fluorophore and consequent emission is on the order of a microsecond, allowing many excitation and emission events

to occur over the course of a single image, which is often on the order of tenths of seconds. See Fig. 2.12 for a timelapse image of two-color fluorescence microscopy.

The emission and excitation wavelength ranges are often distinct from each other, enabling researchers to separate the emission spectra from the excitation spectra. Over time, fluorophores experience a process known as photobleaching, wherein the fluorophore reaches a state where it can no longer be excited and can therefore no longer emit photons. This process can be caused by either chemical damage or photochemical effects from exposure to excitation light. At this point, the fluorophore can no longer be tracked, so information about the protein of interest is lost. This phenomenon limits the time over which we can observe protein localization, and consequently of our data sets are almost exclusively less than ten minutes.

1.5.3 Fluorescent fusions

The gene for the first fluorescent protein (green fluorescent protein, or GFP) was discovered in a bioluminescent jellyfish, *Aequorea victoria* in the 1960s. It was determined that this fluorophore was both viable and able to be excited with light in its emission spectra under standard laboratory conditions [62]. Since then, more fluorophores used for labeling proteins have been discovered or developed. mCherry is one common fluorophore not derived from GFP, but rather isolated from *Discosoma sp.*. The DNA for some fluorophores, including the ones used in this study, may be genetically attached to the DNA of the protein of interest and thus the fluorophores are produced by bacterial cells each time they construct the protein of interest. GFP and mCherry fusions, among other fluorophores, have been expressed in this way in many organisms beyond bacteria and are well-established as protein labeling schemes.

The main drawback of this labeling scheme is that adding the bulky fluorescent label to the protein of interest may diminish or completely negate the normal function of the protein. Thus, it is always important to test the functionality of the protein within the cell

to determine whether the protein retains its normal operation after labeling.

It is often helpful to track two proteins simultaneously or near-simultaneously in order to analyze the interactions of these proteins. To label two proteins at once, two fluorophores must be used. A common combination of fluorophores is GFP and mCherry. The excitation and emission spectra for GFP and mCherry are distinct (GFP excitation and emission: 475-495 nm, 520-560 nm; mCherry excitation and emission: 540-580 nm, 600-680 nm). This allows us to excite each protein individually and apply filters on detected light to only record light in the emission spectrum of the relevant fluorophore. In this way, we can identify and track multiple proteins in the same cell and cell population.

1.5.4 Diffusion

Fluorescence from protein not bound in a complex appears focused, whereas fluorescence from unbound protein is dispersed throughout the cytoplasm and consequently appears diffuse. The diffusion coefficient (D) for a spherical particle is given by the Stokes-Einstein relation,

$$D = \frac{kT}{6\pi r\eta} \tag{1.1}$$

and depends on the temperature (T), radius of the particle (r), and the viscosity of the surrounding medium (η). Boltzmann's constant is indicated by k. An estimate of the diffusion constant for a standard globular protein in water is roughly 100 μm^2/s [50]. Given this equation, the standard time (t) for a molecule to travel a distance d is approximately

$$t \approx d^2/D \tag{1.2}$$

The long axis of a *P. aeruginosa* cell is typically about 2 μm in dimension. Therefore, the average time for a protein to diffuse along the length of an entire cell is $\approx$ 40 ms. Exposure times for this study were in the 500-900 ms range, meaning that fluorescence from unbound protein had more than sufficient time to blur across the image during the time of exposure. The background fluorescence produced by rapidly diffusing proteins, as well

as produced by the autofluorescence of water, is subtracted from the measured intensities of protein foci. In this way we ensure that that intensity traces of bound proteins, which we identify by locating punctate foci in the fluorescence image, only measure the change in intensity of the focus and not changes in background intensity.

1.5.5 Diffraction limit

Although bacterial proteins are able to be identified and tracked via fluorescence microscopy as described above, the resolution of the subcellular structures created by this bound protein is fundamentally limited by the physical properties of light. The Abbe diffraction limit for a microscope is:

$$d = \frac{\lambda}{2n \sin \theta} \tag{1.3}$$

The $n \sin \theta$ portion of the equation is known as the numerical aperture (NA) and depends on the particulars of a given microscope. In modern microscopy, the numerical aperture is often around 1.4-1.6. This limits the resolution of microscopic objects to roughly 200 nm. Practically speaking, foci must be 200 nm apart from each other to be distinguished, and the structures which comprise the foci must be greater than 200 nm to be resolved. Objects on the scale of bacterial cells, which have a length scale on the order of μm, but subcellular objects, including proteins which are on the order of nm, are below this diffraction limit. This lower limit could be decreased by using light wavelengths in the UV and X-ray spectrum, but light in this spectrum tends to damage the sample and lack desired contrast. Other techniques have been discussed in the literature for reducing the diffraction limit, but in general, basic fluorescence microscopy cannot resolve structures below this limit [32]. This limit becomes particularly important in this work when investigating the T6SS mechanism of effector delivery in *P. aeruginosa*.

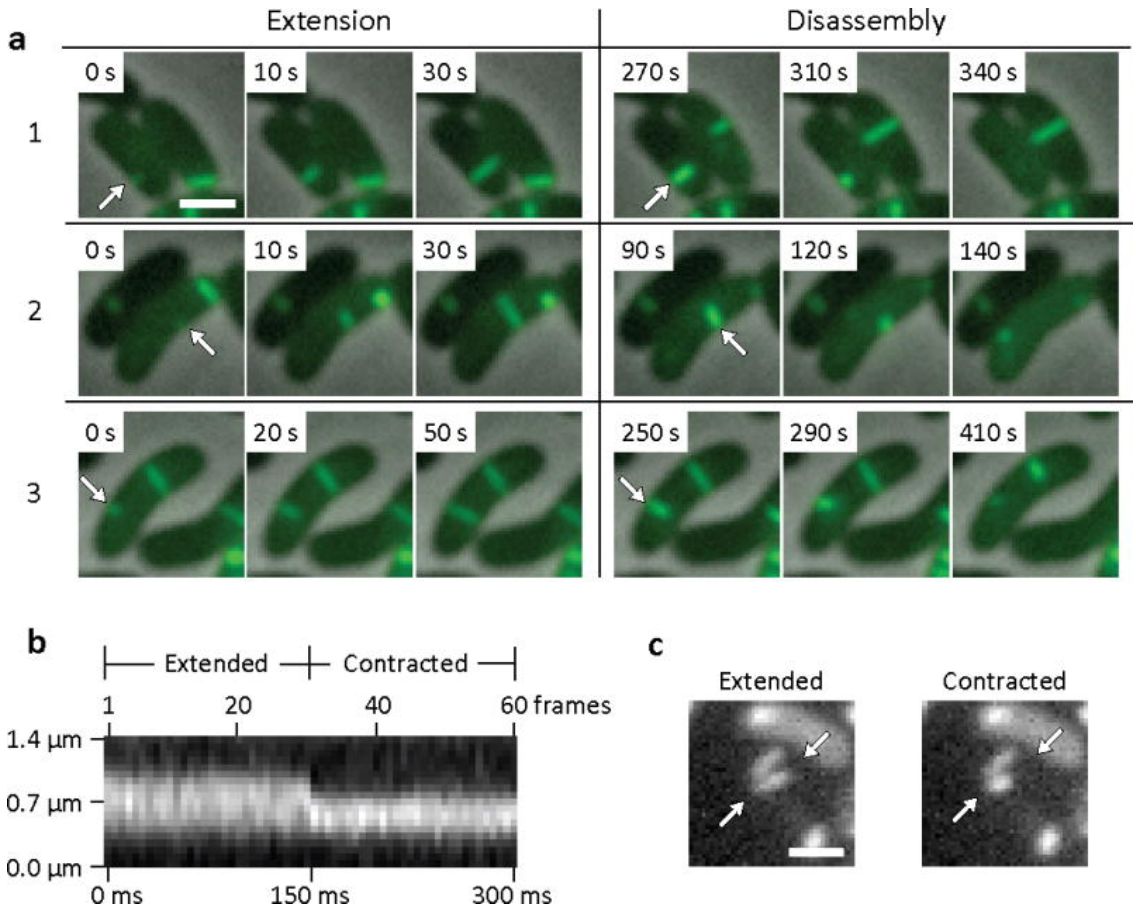

Figure 1.1: **Fluorescence light microscopy of TssB-sfGFP** (a) Individual 33 m frames from a time-lapse imaging with a frame rate of 10 sec per frame show 3 frames of extension of TssB-sfGFP structure in TssB background from one side of the cell to another (arrows) followed by a contraction event and apparent disassembly (shown on 3 frames) of the contracted TssB-sfGFP structure (arrows). Bar shown on the first frame represents 1 m. (b) Kymogram illustrating rapid change in the length of TssB-sfGFP structure. Projection of signal intensity in time at a rate of 200 frames per second along the axis of the maximal intensity on an extended structure (30 frame average shown on the panel (c) left) showing a contraction in length and increase in maximal intensity of the contracted structure (30 frame average shown on the panel (c) right). Arrows indicate contracting TssB-sfGFP structure and mark start and end of a line for generating the kymogram. Bar shown on the average frames is 1 m long. Gaussian blur filter (sigma radius = 1) was applied to individual frames prior to generating the kymogram. Taken from [7], permission pending.

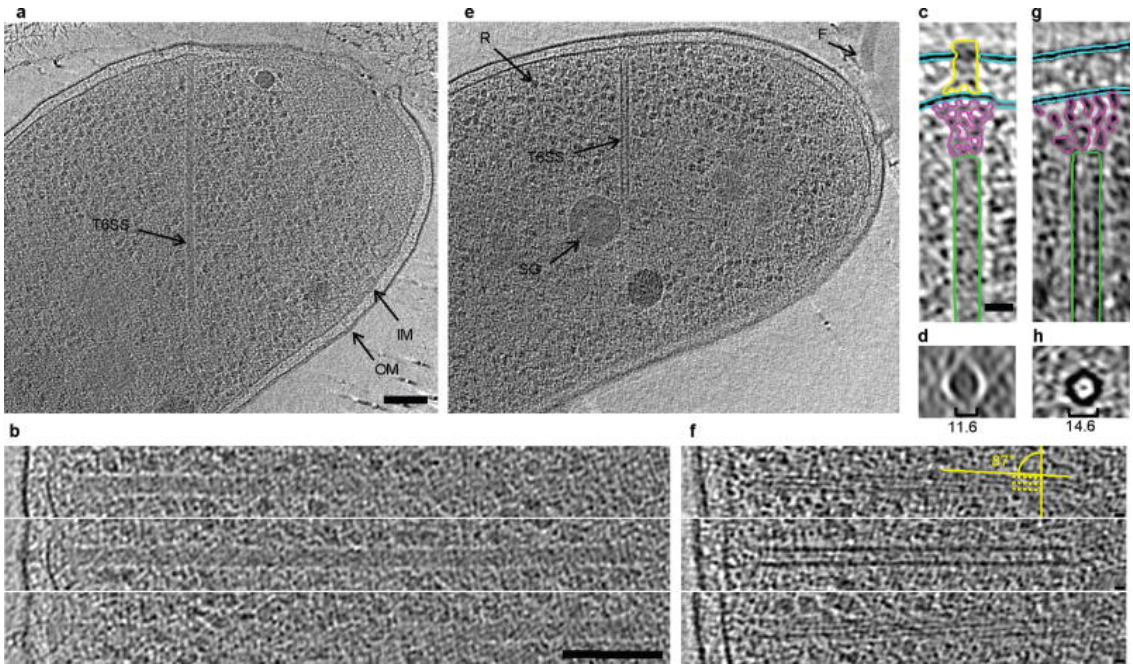

Figure 1.2: **Electron cryotomographic imaging of T6SS structures inside intact cells** Shown are different tomographic slices (19 nm in a, e, c, g; 9.5 nm in b,f; 190 nm in d, h) of an extended (ad) and a contracted (eh) structure imaged in two different wild type cells (contracted/extended structures, T6SS; IM, inner membrane; OM, outer membrane; F, flagellum; R, putative ribosome; SG, polyphosphate storage granule). (b) and (f), each show three slices at the same orientation but at different Z-heights. Compared to extended structures, contracted structures are shorter (b, f), have a helical surface pattern (pitch angle of 87) and a smaller diameter (indicated in the perpendicular views in d, h). (c) and (g) are segmentations of densities observed in the extended (c) and contracted (g) structures. Densities shown in (h) originate from a contracted structure from a different tomogram. Segmented are putative densities corresponding to sheath (green), baseplate (pink and yellow) and membranes (blue). Bar in (a) 100 nm (applies to a, e), bar in (b) 100 nm (applies to b, f), bar in (c) 20 nm (applies to c, d, g, h). Taken from [7], permission pending.

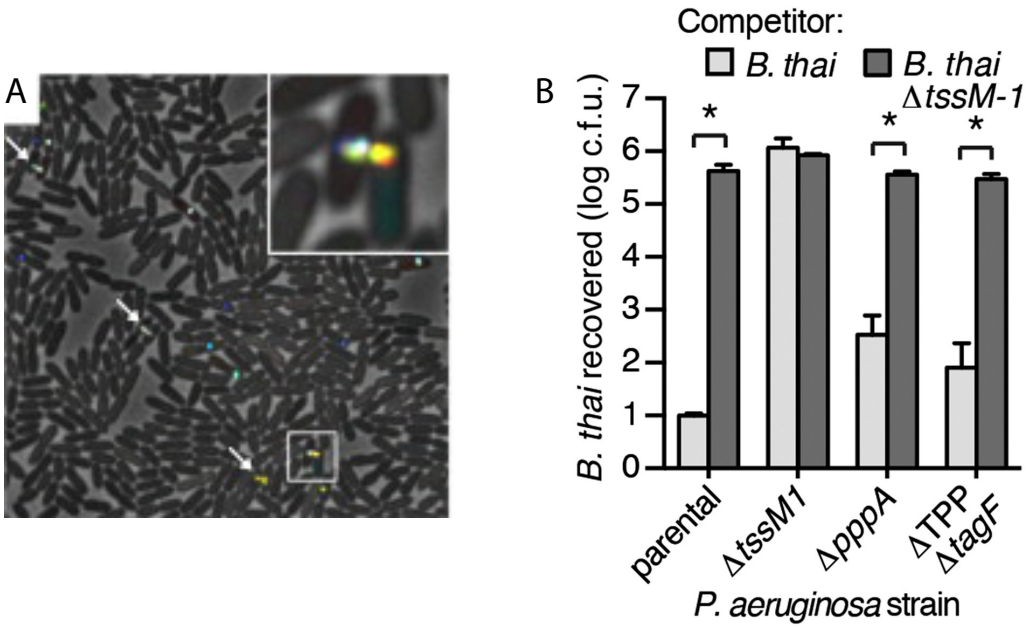

Figure 1.3: Sample data demonstrating current methods of measuring T6SS targeting. **Panel A:** ClpV-GFP localization was followed for 3 min and was temporally color coded. Arrows point to examples of dueling *P. aeruginosa* cells. 30 30 m. **Panel B:** Outcome of growth competition experiments measuring survival of *B. thailandensis* following co-culture with the indicated *P. aeruginosa* strain under T6SS-promoting conditions. Error bars represent ±SD; n = 3 co-cultures. Taken from [8, 41]. Permission pending.

Chapter 2

T6SS DYNAMICS REVEALS A NOVEL SECRETION MECHANISM IN *Pseudomonas aeruginosa*

Portions of this chapter are currently in the revision process for submission.

2.1 Abstract

The Type VI Secretion System (T6SS) inhibits growth of neighboring bacterial cells by secreting effectors by a contact-mediated mechanism. A secretion mechanism has been proposed for *Vibrio cholerae*. We report that the observed T6SS protein localization dynamics in *Pseudomonas aeruginosa* is inconsistent with this proposed model. In *P. aeruginosa*, coordinated assembly and disassembly of diffraction-limited foci of TssB and ClpV are observed without the signature of TssB contraction, in contrast to *V. cholerae*. Motivated by the phenomenon of dynamic instability, we propose a new model in which ATP hydrolysis, rather than conformational change, generates the force for secretion. Genetic evidence suggests this new model may describe T6SS function in many Gram-negative bacteria.

2.2 Introduction

Bacteria compete against neighbors for resources including nutrients and habitat. Many bacterial species have consequently developed mechanisms to increase their relative fitness in competition with neighboring cells. One prevalent mechanism is the type six secretion system (T6SS), found in about a quarter of Gram-negative bacteria, including *Pseudomonas aeruginosa* and *Vibrio cholerae*. This secretion system delivers toxic effectors to neighboring bacteria, causing lysis or cessation of growth [15, 57].

A model for T6SS toxin delivery has been built primarily using observations in the *V. cholerae* T6SS (Fig 2.1). In the *V. cholerae* model, two proteins (TssB and TssC) complex in the cytosol to form a tubular sheath which contracts, forcing the T6SS spike and inner tube complex out of the donor cell [7]. Disassembly of the contracted sheath in the cytoplasm is carried out by ClpV, an AAA+ adenosine phosphate (ATPase) [7]. In *V. cholerae*, ClpV interacts through its N-terminal domain with only the contracted form of the TssBC complex, remodeling the tubules formed by that complex [10, 6]. $\Delta clpV$ strains have a partial loss-of-function of T6SS, demonstrating ClpV to be an important yet non-essential component of T6SS in *V. cholerae* [10, 35, 40].

Previous papers have noted that in *V. cholerae* TssBC extension and contraction are above the diffraction limit, happen one time at one location, and that ClpV interacts with TssC only when the TssBC sheath has contracted [6, 8]. Such observations have led to a syringe-like model of force generation for toxin delivery, where TssBC sheath contraction provides the force to push the inner needle out of the cell and ClpV's role is solely to disassemble the sheath after contraction. In contrast, in the H1-T6SS of *P. aeruginosa* and *Serratia marcescens* (another bacterial species with a well-characterized T6SS), both TssB and ClpV frequently oscillate between diffuse and punctate foci in the same location before final disassembly, suggesting TssB and ClpV interact differently in these systems than in the *V. cholerae* T6SS [22]. Additionally, the N-terminus of ClpV in *P. aeruginosa* does not interact with TssC, and it seems likely that the interaction between TssC and ClpV is mediated by TagJ [22, 20]. Despite these indications that function of essential T6SS proteins fundamentally differ between species, no in-depth study has been performed to specifically test the consistency of the *V. cholerae* model of T6SS in other bacterial species. The homology between most required proteins has suggested that T6SS function would remain qualitatively the same throughout bacterial species. However, despite this homology, some key differences in behavior have been observed.

Due to the stochastic nature of the secretion-system assembly and disassembly at subcellular positions, quantitative analysis is necessary to distinguish T6SS behavioral dif-

ferences between species. We focused on characterizing *P. aeruginosa* H1-T6SS dynamics to define the differences between this system and the well-characterized *V. cholerae* T6SS. To do this, we imaged fluorescent fusions to T6SS proteins to visualize protein localization and dynamics. The relative occupancy for a fusion can be measured by focus intensity. We investigated dynamics of three important H1-T6SS components which have also been characterized in other well-characterized T6SSs: ClpV, TssB, and Fha. ClpV has frequently been used to study H1-T6SS in prior studies, and ClpV foci have been shown to correlate with T6SS-dependent cell-killing [47, 35]. TssB has been studied by Basler *et al.* in combination with ClpV in *V. cholerae*, and we investigate these proteins in *P. aeruginosa* for direct comparison [6]. Fha has been shown to recruit downstream proteins to the H1-T6SS apparatus [31, 43]. It is hypothesized to be a component of the T6SS baseplate, arriving upstream of ClpV in T6SS assembly [46]. Although it is essential in H1-T6SS, it has no analogue in half of all discovered T6SSs, and is absent in *V. cholerae* but is present in *S. marcescens* [12, 44]. Prior to this paper, the dynamics of Fha had not yet been investigated; in this study, we also present the first visualization of T6SS Fha dynamics in any bacterial species, adding important context for the delivery mechanism.

This fluorescence microscopy data analysis combined with prior research into the H1-T6SS of *P. aeruginosa* and other T6S systems indicates that the differences in function in different T6S systems are beyond peripheral. We present a new model for T6SS toxin delivery which describes toxin delivery and sheath contraction using a pump model rather than a syringe contraction.

2.3 Results

2.3.1 ClpV rapidly assembles and disassembles multiple times at the same location

We initially focused on ClpV localization dynamics. ClpV is a member of the AAA+ ATPase protein family which is an essential component of the T6SS [60]. AAA+ proteins typically assemble into oligomeric ring-like enzyme machines that generate mechanical force

by ATP hydrolysis and are known to remodel a variety of substrates [25]. In *V. cholerae*, ClpV is known to disassemble the TssBC sheath after sheath contraction [6]. It is already known that the activation and dynamics of ClpV in *P. aeruginosa* are qualitatively different from *V. cholerae*. Although the T6SS is constitutively active in *V. cholerae* as identified by the localization of T6SS proteins [6], in *P. aeruginosa* the ClpV of H1-T6SS rarely localizes unless it is specifically activated [46].

In *P. aeruginosa* ClpV forms a focus and is pulse-like in intensity in the same location before final disassembly, although this pulsation has not been quantified prior to this study. Additionally, data from Basler *et al.* demonstrates that labeled *V. cholerae* ClpV foci can move in the cell prior to disassembly while assembled *P. aeruginosa* ClpV foci remain stationary [6]. Although *P. aeruginosa* ClpV foci can appear in new locations in the cell, these foci are always assembled at these new locations, rather than moving as an assembled complex, as is observed in *V. cholerae* [6].

To make a quantitative comparison between ClpV dynamics in *P. aeruginosa* and the dynamics reported for *V. cholerae*, we measured ClpV focus intensity over time. (Figs. 2.9 and 2.2.) We observed repeated ClpV localization-delocalization events in quick succession in the same location, followed by long pauses. We call individual events *spikes* and a cluster of spikes *a firing event*. (Fig. 2.2A.) To analyze these intensity traces, we segmented the trace into two states based on the focus intensity: *assembled*, corresponding to a ClpV focus, and *disassembled*, corresponding to background intensity (SI: Fig. 2.11). We then quantified the lifetime of the observed states and the number of spikes per firing event. A histogram of both the spike lifetimes and the pauses, the duration between spikes, is shown in Fig. 2.2B.

In wild type strains, ClpV firing consisted of a group of one to eight spikes with a mean of 2.0 spikes per firing event. The ClpV foci remained stationary throughout firing. The spikes had a mean lifetime of 37 s and a median pause of 33 s between ungrouped spikes. Grouped spikes had a median pause less than our frame rate of 5 s. After the last delocalization event, the intensity returned to cell background intensity, as seen in Fig. 2.2A. In

V. cholerae, firing events correspond to a single spike and therefore the repeated spiking at a fixed location observed in *P. aeruginosa* is an important qualitative distinction between the two T6S systems [6]. Interestingly, in spite of this qualitative difference, the average lifetime of one ClpV event in *V. cholerae* and *P. aeruginosa* is nearly identical (34 s and 37 s, respectively).

To compare the activity of the T6SS between *V. cholerae* and *P. aeruginosa* we estimated the overall firing rate between the two species. In wild type *P. aeruginosa* cells, we observe that just 11.3% of cells contain a ClpV focus over a 7 min experiment, consistent with a firing rate of 0.01 spikes/cell/second. At any time, 1.4% of cells had a ClpV focus. In wild type *P. aeruginosa* cells, 0.3% of cells have two or more firing locations. In 11% of cells, a second firing event occurs in the same location as the original, as measured by a firing event occurring a minute or more after firing has ceased. This indicates that the T6SS apparatus does not always fully disassemble after firing, but sometimes can reinitiate T6SS activity at that same location.

In contrast, $>$90% of all *V. cholerae* cells were observed to have a T6SS focus, and many cells were observed to have two or more firing events [6, 35]. However, in *V. cholerae*, there is only one firing event at each location [6].

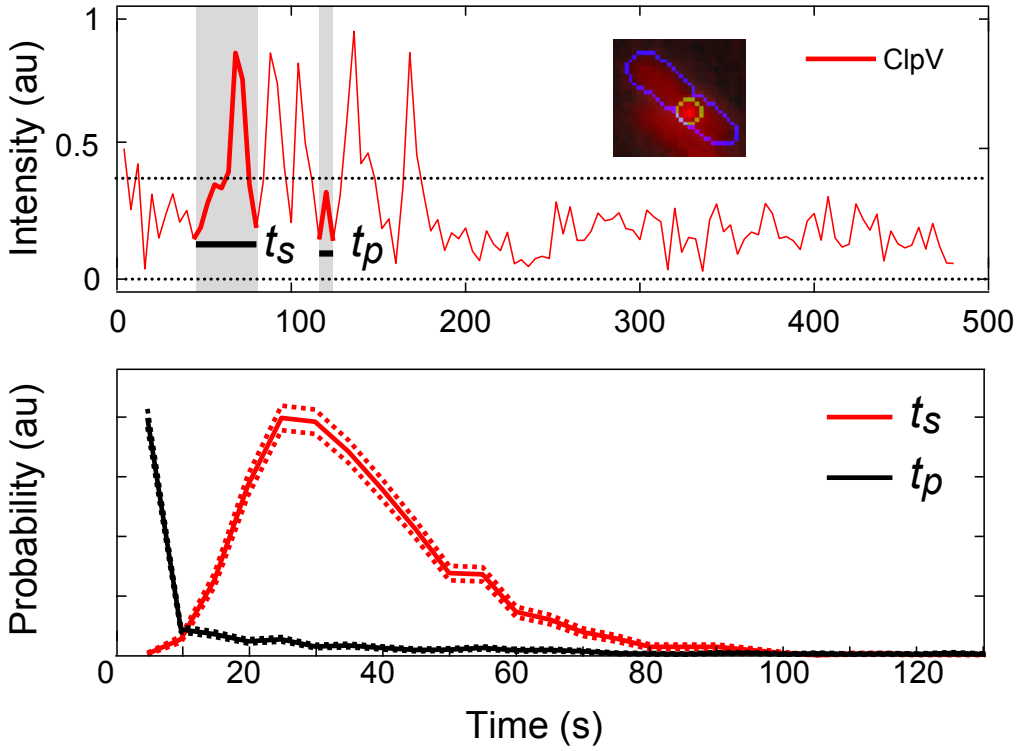

Figure 2.2: Example data demonstrating measurement of ClpV firing lifetimes, t_s, and time between firing events, t_p. There are five firing events in this trace. **Top:** Representative ClpV firing for a single cell at one focus region. Inset shows image of cell with focus area indicated by outline. For now and each figure afterward, each trace is representative of one focus area in one cell. **Bottom:** Comparisons of ClpV lifetimes. Mean lifetime is 37 sec. $n \approx 2200$. Measurement of time between spikes. $n \approx 1100$.

2.3.2 *TssB contraction events are not observed in P. aeruginosa*

Having characterized ClpV dynamics, we next performed a detailed analysis of the dynamics of the TssB protein, a component of the T6SS sheath [10]. TssB is an essential component of T6SS and in *V. cholerae* is known to assemble into tubules with TssC [10]. In *V. cholerae*, these tubules have both an extended and contracted form, assembling in the extended form then spontaneously contracting [7]. This contractile-tubule sheath has been hypothesized to be the effector delivery mechanism. After effector delivery, the

contracted tubule is depolymerized by ClpV and sheath components are recycled [7, 10]. However contraction has not been observed in other bacteria. For instance, although the sheath has been visualized by fluorescence microscopy in *S. marcescens*, the contraction has not been observed [6, 22].

In close analogy to the observations in *S. marcescens*, we observed TssB foci in WT *P. aeruginosa* and determined that these foci were below the diffraction limit (Fig. 2.3A) and therefore no contraction events could be resolved. The rare exception was in the $\Delta retS$ background in *P. aeruginosa*; in less than one-tenth percent of these cells, we observed an extension of ClpV or TssB across the width of the cell. This suggests that in rare circumstances, the TssB sheath can lengthen above the diffraction limit, and ClpV can extend as well. These observations do not recapitulate the dynamics observed in *V. cholerae*, where extended sheaths consistently have lengths around 0.75-1 m which contract to roughly 50% of their extended length [7]. This sheath length allows for the *V. cholerae* model, which is dependent on a sheath large enough to load an inner needle that can reach and penetrate a neighboring cell after one sheath contraction. However, since the diffraction limit is approximately 0.2 m, the TssBC structure in *P. aeruginosa* is at most 25% the length of the *V. cholerae* TssBC structure. This much shorter length of the *P. aeruginosa* TssBC structure does not satisfy the sheath length requirement of the *V. cholerae* model, suggesting another mode of delivery must be employed in *P. aeruginosa*.

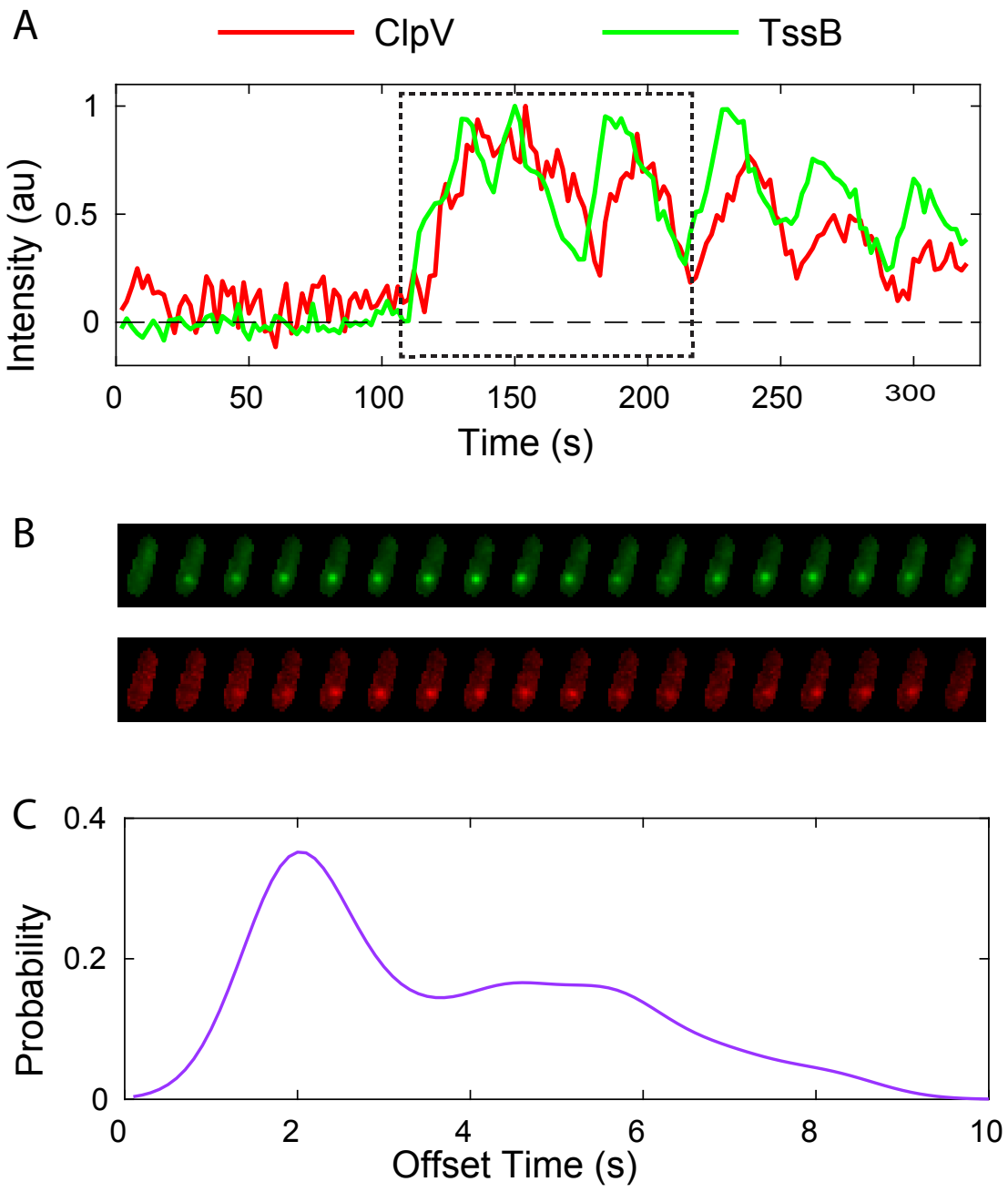

Figure 2.3: **Panel A:** TssB (top) and ClpV (bottom) localization over time in single cell. 2 s frame rate. Fluorescent intensity fluctuates and focus motion is observed but the focus remains diffraction-limited. Cell images for the region indicated by the dashed boundary are shown in Panel B. **Panel B:** Typical single focus data shows a representative coordinated ClpV and TssB fluorescence intensity traces for one focus region in Δ*retS* background. **Panel C:** Population-level analysis reveals average lag times between ClpV and TssB traces.$n \approx 280$.

2.3.3 TssB and ClpV localization dynamics are coordinated, not sequential

Using two-color imaging of TssB and ClpV in *V. cholerae*, Basler *et al* were able to observe the sequential process of sheath assembly (TssB), contraction, ClpV localization and disassembly [6]. The syringe model predicts that analogous dynamics should be observed in *P. aeruginosa*.

To characterize the coordination between TssB and ClpV in *P. aeruginosa*, we initially investigated the ClpV-mCherry/TssB-GFP localization in the Δ*retS* background, in which H1-T6SS is constitutively active. RetS is a post-transcriptional regulatory protein which downregulates T6SS activity [71].

It is important to note that in both wild type and Δ*retS* backgrounds, the ClpV-mCherry/TssB-GFP double fusion measurably changed ClpV behavior compared to the ClpV-mCherry fusion alone. Although ClpV-mCherry focus lifetime is identical in both strains, the ClpV-mCherry/TssB-GFp foci lifetimes are 10% longer in Δ*retS* where T6SS is overexpressed. In wild type, this fusion had a significantly diminished firing rate, with at most one ClpV/TssB firing event seen over the 7-9 minute experiment with a spike lifetime 5x as long as wild type ClpV-mCherry. Due to these observations, we believe the qualitative localization dynamics observed in ClpV-mCherry/TssB-GFP Δ*retS* is informative.

Both the ClpV-mCherry and TssB-GFP fusions formed foci that were observed to co-localize and to undergo very similar (and correlated) dynamics, as shown in Fig. 2.3A and B. Consistent with the syringe model in which ClpV disassembles the TssBC sheath, the ClpV intensity profile (localization) in *V. cholerae* was observed to lag behind the TssB intensity profile - ClpV localizes to the TssBC sheath 5-10 s after sheath contraction [6, 7]. In *P. aeruginosa*, we observe that the ClpV and TssB intensity profiles were nearly identical except for a short lag in the ClpV localization profile, as shown in Fig. 2.3B. To quantify the lag time, we calculated the cross-correlation between the TssB-GFP and ClpV-mCherry fluorescence. The mean lag time was found to be 2.7 s (Fig. 2.3C).

In contrast to the syringe model which predicts sequential dynamics, the similarity

between the TssB and ClpV localization profiles is consistent with coordinated dynamics or a leader-follower mechanism. An interesting contrast between the dynamics in *P. aeruginosa* and *V. cholerae* is that lag time: In *V. cholerae* there is a 100–200 s lag between TssB assembly and ClpV localization and the localization. Furthermore, in *V. cholerae*, the localization profiles of TssB and ClpV are distinctly different [6].

2.3.4 Fha localization precedes and remains throughout ClpV activity

After observing the close coordination between TssB and ClpV, we wished to determine whether this coordination was specific to sheath and sheath-associated proteins or representative of all T6SS proteins. We therefore investigated the localization dynamics of the upstream T6SS-essential protein Fha. We constructed a double-labeled ClpV-mCherry/Fha-sfGFP strain and observed the localization dynamics of both proteins (Fig. 2.4). Fha has qualitatively different localization dynamics from either ClpV or TssB. Fha was observed to localize and delocalize gradually, making it difficult to consistently classify the dynamics using a method analogous to that used for ClpV and TssB. Although Fha does not spike, its persistent localization appears to be essential for ClpV localization since ClpV firing was never observed without Fha localization. Furthermore, Fha enveloped the ClpV spikes: out of approximately 1800 observations, Fha always appeared before ClpV firing, was retained throughout and disassembled after the end of the firing event, consistent with its proposed role as part of the T6SS baseplate complex [46]. Therefore, the close coordination between ClpV and TssB localization patterns appears to be specific to the sheath and not to H1-T6SS proteins in general.

Fha appeared on average 20 s before ClpV began to spike. Given this information, the correspondence between TssB and ClpV behavior, and the loss of function with the TssB label, we did not label Fha and TssB together; we can ascertain without experiment that Fha also envelopes TssB behavior.

2.3.5 *Focus movement is linear and normal to cell membrane*

CryoEM images have shown that the T6SS in *V. cholerae* forms a sheath roughly perpendicular to the cell membrane which is large enough to be resolved by fluorescence microscopy [7]. The sheath contraction can also be directly visualized. Due to the small size of the *P. aeruginosa* TssB and ClpV foci, no direct motion or TssBC contraction has yet been observed in *P. aeruginosa*, but the movement of the focus can be tracked to a higher resolution than the diffraction limit. We therefore tracked ClpV foci in *P. aeruginosa* H1-T6SS with 5 s time resolution to determine whether the observed motions were consistent with sheath contraction. (The resolution for tracking foci was determined to be 50 nm, limited by the non-uniform fluorescence background due to the cytoplasmic fluorescence.) We chose to track ClpV foci rather than TssB foci because we had determined that ClpV and TssB foci have near identical behavior, yet the fluorescent labeling of TssB tended to disrupt H1-T6SS dynamics to a greater extent than the labeling of ClpV. Thus, investigating the dynamics of ClpV foci minimized the disruption to the system caused by fluorescent labeling while still being representative of key dynamic components of the H1-T6SS.

To probe whether the motion was consistent with a sheath with a length that varied over time, we first investigated whether the observed motions of the protein foci were better modeled by isotropic or anisotropic random motion. Sheath contraction would result in anisotropic motion due to the increased variance along the axis of sheath due to contraction. To measure the anisotropy, we calculated an anisotropy score for each trace by finding the eigenvectors of the covariance matrix of the focus position, then determining the ratio of the maximum and minimum eigenvalues. A high ratio would indicate strong anisotropy, while a ratio close to one would indicate isotropy. To determine the significance of the anisotropy, we computed the test statistic by simulating the distribution of the anisotropy score for a two-dimensional normal distribution with an isotropic covariance matrix with the same number of observations as the focus trajectory. An example of measured and random data in context of a cell is shown in Fig. 2.5A.

We found that the anisotropy score was too large to be described by isotropic random motion: 45% of the measured data had a anisotropy score higher than the 95% confidence level. Using the Fisher test, we combined these measurements to generate a single p-value which is less than 0.0001, which rejects the null hypothesis that the distribution of positions is isotropic. (If the anisotropy score were due to statistical fluctuations we would expect just 5% of score to exceed the 95% confidence level.) Although the anisotropy of the motion is clearly statistically significant, it is not large. The mean range of ClpV movements was 300 nm.

Finally, we investigated the orientation of ClpV movement relative to the cell membrane. For each focus, we determined the normal to the cell membrane and the best-fit line of ClpV and calculated the angle between them. We discovered that, compared to random, the slope of the ClpV best-fit line was about six times as likely to be within 10° of the normal, indicating strong perpendicularity. Like the *V. cholerae* syringe model, this apparatus is also optimally oriented to deliver toxins outside the cell.

2.3.6 ClpV motion correlates with ClpV intensity

We hypothesized that a change in the length of the sheath would correspond with both focus movement as well as a change in fluorescent intensity. We therefore posited that focus motion corresponds with changes in the length of the sheath and that that rapid changes in motion correspond to fluctuations in intensity. In order to calculate the significance of this relationship, we calculated Pearsons correlation coefficient for each data set. We noted that significant increases in speed corresponded with both increases and decreases in fluorescent intensity (Fig. 2.5A and C).

This result is clearly discrepant with the *V. cholerae* syringe model. In the syringe model, effector delivery is driven by sheath contraction that occurs due to a cooperative conformation change in TssBC. The length of the sheath is reduced without reducing the number of proteins. Therefore, contraction is expected to lead to a rapid change in the

focus position without a change in the focus intensity. However, in contrast, manual inspection of the intensity and position traces in *P. aeruginosa* demonstrated that significant changes in position of the TssB focus were accompanied by changes in intensity. Therefore, even with sub-diffraction limit tracking of the centroid of the sheath, we found no clear evidence for contraction events in *P. aeruginosa*.

In contrast, the pump model includes a mechanism where movement of the focus centroid corresponds with amount of protein present. In the pump model, the center of the focus moves as the TssBC sheath (and the corresponding ClpV) both grows and shrinks. Our observations are consistent with this prediction, indicating effector delivery often happens over the course of several closely-timed ClpV spikes, rather than in the one swift contraction of the *V. cholerae* model.

Because of the clear relation between focus intensity and movement in both ClpV and Fha, we looked for correspondences between these quantities in each protein. We found that while ClpV and Fha intensities had a weak correlation, there was no correlation between ClpV and Fha positions or speeds.

2.3.7 Distances between focus centroids indicate separation of proteins

Even though the T6SS complex is itself diffraction limited, the extended nature of the ClpV complex is expected to shift the ClpV focus centroid relative to the Fha focus centroid. In all strains, the distance between the mean centroid position of ClpV and Fha was 100 nm.

The fluctuations in the displacement of the centroid was dominated by the movement of the ClpV focus which is large compared with the movement of Fha. (See Fig. 2.7, Fig. 2.6.) If Fha is associated with a membrane-bound complex and ClpV coats the surface of a tubule extending at a normal angle from the base, the displace between centroids would be aligned with the transverse axis of the cell.

The observed displacement between the ClpV and Fha centroids was not always aligned

with the transverse axis of the cell. (See Fig. 2.7.) This observation is consistent with our previous data on the collinear centroid dynamics, which also does not always align with the transverse axis of the cell. These observations suggest that either the tubule itself or its attachment with the base plate are flexible.

ClpV dynamically moves along the sheath and we were unaware of any precedent for dynamic movement of Fha, we anticipated that the proteins would be a small distance apart. Given the motion of ClpV at the beginning and end of firing events, we also hypothesized that if we looked at each time point, we would have a bimodal distribution of ClpV-Fha distances. We compared both the average distance of ClpV and Fha over the lifetime of the focus, as well as the distance between ClpV and Fha at each time point. In all strains, the distance between ClpV and Fha averaged over time was 100 nm, but when measuring at each time point, the average distance was 150 nm. In contrast to our hypothesis, both distributions were normal.

2.4 Discussion

2.4.1 TssB, ClpV and Fha exhibit distinct dynamics

TssB, ClpV, and Fha exhibit distinct dynamics. ClpV localization transitions between diffuse to a single punctate focus. In general, no extended period of constant intensity is observed for ClpV foci. TssB dynamics are nearly identical to ClpV dynamics, and lead the ClpV intensity by 2-3 s. Because the ClpV intensity trace so closely follows the TssB intensity trace, ClpV is a useful proxy for understanding the dynamics of the T6SS TssBC sheath. The appearance of TssB localization before ClpV localization is consistent with the proposed role of ClpV in disassembling the TssBC sheath.

Like TssB, Fha is also observed to co-localize with ClpV, but in contrast to both TssB and ClpV, Fha is significantly less dynamic. The duration of delay between Fha and ClpV localization relative to TssB and ClpV suggests that Fha always localizes before TssB. These observations are consistent with the role of Fha in a process upstream of sheath

formation, possibly including ClpV recruitment [31].

To test the dynamic sheath model, we tracked the motion of ClpV. The T6SS model predicts ClpV focus position should rapidly oscillate normal to the membrane since it is associated with the sheath. ClpV foci motion is collinear, consistent with the hypothesis that ClpV moves along the linear TssBC sheath as part of the disassembly process. Additionally, motion of the ClpV focus corresponded with intensity of the focus, indicating that changes in the location of the ClpV centroid correspond with the amount of ClpV present at the focus.

2.4.2 Evidence for a novel secretion mechanism

Although it would be natural to expect an analogous secretion mechanism in the *V. cholerae* and *P. aeruginosa* T6SSs, our analysis reveals striking quantitative and qualitative differences in both TssB and ClpV dynamics and structure. In *P. aeruginosa*, ClpV intensity traces resemble *triangle-waves*: the intensity first undergoes steady growth then steady decay and closely follows an analogous pattern in the TssB trace. Several of these spiking events may occur in close succession. In contrast, in *V. cholerae*, the ClpV intensity resembles a single *square-wave*: ClpV rapidly localizes and then de-localizes, but only after TssBC contraction is observed. In this case, ClpV and TssB localization is sequential, rather than coordinated, and only a single spiking event is observed during firing. The rapid localization of ClpV to the assembling sheath, the repeated spiking, and the absence of detectable sheath contraction all conflict with the proposed syringe model and the observed dynamics in *V. cholerae*.

In addition to the differences in dynamics, there are cellular-scale differences in the T6SS structure. In *P. aeruginosa*, the TssB focus is diffraction-limited, but is optically resolvable in *V. cholerae*. The greatly reduced size of the *P. aeruginosa* H1-T6SS may require repeated secretion events to secrete the same number of effectors as the *V. cholerae* T6SS, consistent with our observations of multiple spikes per firing event.

There is also precedent for mechanistic distinctions in the constituent proteins and characterized protein interactions. In *V. cholerae* there is a well-characterized and direct interaction between ClpV and TssC: once the TssBC sheath contracts, the N-terminal ClpV-binding domain of TssC is exposed, facilitating sheath disassembly. In *P. aeruginosa*, no such direct interaction between ClpV and TssC has been observed [6, 44]. Rather, in *P. aeruginosa* ClpV and TssB interactions are mediated by TagJ and do not appear to be dependent on sheath contraction [44]. Together, the differences in T6SS dynamics, sheath size and protein function are consistent with the existence of a distinct secretion mechanism in *P. aeruginosa*.

2.4.3 The pump model and a dynamic instability

The mismatch between the dynamics predicted by the syringe model and the observed phenomenology motivates the consideration of alternative models for secretion and force generation in the T6SS. In particular, the sheath contraction of the *V. cholerae* T6SS is hypothesized to be a principle mechanism responsible for puncturing the cell wall of the neighboring cell. During the contraction, the *V. cholerae* sheath contracts to half its length *without de-polymerization*, but we could not detect sheath contraction in *P. aeruginosa*. Instead, the *P. aeruginosa* sheath alternates between growth and decay states (*i.e.* changes in length due to change in the number of protein subunits). We propose that this observed growth and decay plays a central role in the secretion process. It is interesting to speculate that the disassembly of the TssBC sheath, driven by ClpV, could provide the force required to secrete the effectors.

It is known that the assembly and disassembly of cytoskeletal filaments can generate force. For instance, microtubule disassembly is responsible for the generation of force on chromosome centromeres during metaphase. Even in *in vitro* reconstitution, purified tubulin can assemble into microtubules that transition between growth and and rapid decay due to phenomena called *dynamic instability*, in which the GTP-hydrolysis front

catches the filament tip.

In the context of T6SS, the growth rate of the TssBC filament is observed to transition back and forth between growth and decay states. Since the filaments do not decay in the absence of ClpV ATPase activity and ClpV is known to bind (via TagJ) to TssBC sheath, it is natural to assume that ClpV directly modulates filament growth. The switch between growing and decaying states is caused by GTP-hydrolysis front in the context of microtubules. In T6SS, the switch could be caused by a number of putative mechanisms: (i) The ClpV intensity trace lags TssB intensity trace, motivating a model in which the ClpV coat is the analogue to the hydrolysis front. When the ClpV coat catches the tip of the assembling sheath, the sheath transitions to a decaying state and TssBC subunits are depolymerized by ClpV ATP hydrolysis. (ii) Alternatively, an analogous ClpV ATP-hydrolysis front may exist in TssBC-bound ClpV which propagates through the sheath. Disassembly may be sterically blocked except at the tip. When the hydrolysis front catches the tip, the sheath transitions to the decaying state. This model could result in consistent maximum spike intensity, as shown in Fig. 2.2A, if the assembly is limited by the depletion of cytoplasmic TssBC.

In both models, it is assumed the disassembly of the sheath drives the internal shaft carrying the effects into the neighboring cell, in analogy to the syringe model. Unlike the *V. cholerae* syringe model, where the force required for effector delivery is generated by the conformational change of TssBC, the pump model depends directly on ATP hydrolysis for force generation, as was originally proposed [46]. We hypothesize that the retention of Fha allows the T6SS sheath to assemble and disassemble multiple times at the same location. We therefore call this model a *pump model*, which is capable of delivering sequential secretions of effectors. Our proposed model is described in Fig. 2.8.

2.4.4 T6SS diversity in bacteria

Evidence for distinct mechanisms in *P. aeruginosa* and *V. cholerae* naturally motivate the questions about the diversity of the T6SS mechanisms in T6SS+ Gram-negative bacteria as a whole. Are there two or more classes of T6SS mechanisms? If so, what are the key genetic signatures of these families? To explore the diversity of the T6SS, consider another characterized system, the *S. marcescens* T6SS. The observed diffraction-limited protein localization of TssB and ClpV and genetic evidence (both the presence of Fha and TagJ, which mediates the interaction between TssB and ClpV) suggest the *S. marcescens* T6SS mechanism is more consistent with the *P. aeruginosa* T6SS than the *V. cholerae* T6SS [22, 44]. Initially, we hypothesized that TagJ and Fha might be phylogenetically linked and a proxy for the *P. aeruginosa*-like T6SS mechanism since both genes are absent from *V. cholerae* and present in *P. aeruginosa* and *S. marcescens*. However, *Agrobacterium tumefaciens* T6SS requires Fha phosphorylation but has no *tagJ* homolog [43, 44]. None of these T6SSs appear to be exceptional, as 30% of T6SS have a *tagJ* homolog and 50% of T6SS have a *fha* homolog [12]. Additionally, there appears to be significantly more frequent TssB without ClpV localization in both *V. cholerae* and *S. marcescens* than in *P. aeruginosa*. These distinctions suggest that T6SS function may be diversified beyond the distinct mechanisms observed in *P. aeruginosa* and *V. cholerae*.

2.4.5 Conclusion

We report on a fine-scale analysis of the dynamics of the T6SS in *P. aeruginosa* using quantitative image analysis of single cells. The simultaneous imaging of TssB and ClpV reveal that the localization of these two proteins in *P. aeruginosa* is synchronized rather than sequential, as observed in *V. cholerae*. To accommodate these observations, we proposed a pump model in which effector delivery is powered by sheath de-polymerization in analogy to force generation by cytoskeletal filaments. Structural differences between the TssC proteins in *V. cholerae* and *P. aeruginosa* (and their concomitant interactions with ClpV) is

consistent with the view that the functional mechanism may be distinct in the two organisms. The genetic similarity between the T6SS in *P. aeruginosa* and other Gram-negative bacteria suggest that this pump mechanism may describe the T6SS function in a significant number of other bacteria.

2.4.6 Acknowledgments

PAW and JC acknowledge Robin Kirkpatrick for edits to image analysis code and Brandon Hoang for performing initial Fha experiments. Support for this research is graciously provided by the National Science Foundation Graduate Research Fellowship DGE-1256082 and the National Institute of Health under award number R21 AI 105268-01.

Methods

2.4.7 Strains

Strains used in this study are described in Tab. 2.1. Strains were derived from *P. aeruginosa* PAO1 and *B. thailandensis* E264 [67, 74]. Functional translational fluorescent C-terminal fusions of either superfolder GFP (sfGFP) or monomeric mCherry (mCherry) were generated to TssB, ClpV, and Fha at their endogenous chromosomal loci by allelic exchange, as described in the supplement [41].

2.4.8 Growth conditions and microscopy

All strains were grown overnight from a single colony in Luria Broth (LB) media. Doubling time in liquid media was roughly 30 min. Overnights were diluted 1:10 into fresh media and grown to $OD_{600} \approx 0.8$. (T6SS is less active in log-phase growth [41].) Agarose pads were prepared by pouring 1 mL of growth media and 0.2% agarose into 2 cm $\times$ 2 cm wells cut into a rubber gasket sealed onto a standard microscope slide. We spotted $2\ \mu$L of cells onto dried pads and a cover slip was placed on top of the pad. The entire slide was sealed with VaLP (1:1:1 Vaseline, lanolin, paraffin).

Table 2.1: Strains used in this study

Organism	Genotype	Source
Pseudomonas aeruginosa PAO1	*clpV-GFP*	Mougous *et al.* 2006. Science. 312:1526-30.
	tssB-sfGFP clpV-mCherry	This study
	ΔretS tssB-sfGFP ClpV-mCherry	This study
	fha1-sfGFP clpV-mCherry	This study
Burkholderia thailandensis	*attTn7::Tp-CFP*	LeRoux *et al.* (2015) *eLife*

To study interactions with a second species, we introduced *B. thailandensis*. *B. thailandensis* was distinguished from *P. aeruginosa* by expression cytoplasmic CFP and gating cells on fluorescence levels in the CFP channel. Introducing *B. thailandensis* also has the advantage of activating T6SS in wild type *P. aeruginosa* [41]. Under normal growth conditions, wild type *P. aeruginosa* has about 1-2% of cells with an active T6SS as identified by the presence of a ClpV focus, but upon exposure to *B. thailandensis*, which activates T6SS via '*P. aeruginosa* response to antagonism (PARA), about 10% of cells have a ClpV focus [41]. All wild type cells in this study were activated via PARA to achieve a higher percentage of cells with foci. To activate *P. aeruginosa* via PARA, immediately prior to spotting cells on the s we added 100 L *B. thailandensis* to 100 L *P. aeruginosa* and spun down (3 min 8000 rpm), removed the supernatant, and resuspended the pellet in 40 L fresh LB before spotting.

Under imaging conditions, the average doubling time for cells was $\approx$ 40 min. Fluo-

rescence microscopy was performed on a Nikon-TiE (Nikon, Tokyo, Japan) with environmental chamber using NIS-Elements software. Images were captured on an Andor Neo sCMOS camera (Belfast, Northern Ireland) at either 2 s or 5 s intervals.

To ascertain the functionality of these strains, we performed bacterial growth competition experiments with fluorescently labeled and unlabeled strains with *B. thailandensis* recipients under comparable conditions. T6S-dependent fitness was determined by comparing the ratio of *P. aeruginosa* to *B. thailandensis* before and after 7 hours of co-culture. We found that all strains reduced populations of *B. thailandensis* in a T6S-dependent manner by an order of magnitude.

2.4.9 Quantitative image analysis

Cells were segmented and linked from phase contrast images using our *SuperSegger* segmentation engine [69]. All time-lapse images were aligned to compensate for stage drift. Cell growth was not appreciable over times-lapse experiments, as observed by phase contrast microscopy. Although SuperSegger can identify and track foci, the current implementation identifies foci in each frame and links foci between frames. This approach is problematic for foci that repeatedly appear and disappear, since it can be difficult to ascertain whether a focus is returning to precisely the same location or not. In the current context, foci are imaged over a sufficiently short period that the movement of foci in this system is small ($<$500 nm). We therefore exploited these slow dynamics to track foci which reappear over time. We first averaged over all frames to generate a summed image, then identified loci in this summed image and defined a circular region (radius 500 nm around the focus position) where loci are allowed to move. To compute the focus intensity in each frame, we convolve each image with a disk (radius 300 nm), and define the focus intensity as the maximum pixel value in the allowed region of the convolved image minus the background intensity. We compute the background intensity by averaging over the fluorescence intensity in the cell, having first masked out the focus using the

300 nm radius disk.

2.5 Supplemental Information (SI)

2.5.1 Strain construction

Fluorescent fusions to endogenous genes were constructed as follows: The 500 bp regions flanking the C-terminus (stop codon) of each target gene was amplified. These flanking regions were spliced together using a BamHI site (GGTACC) replacing the stop codon of the target gene. (The BamHI sequence acted as a two residue linker between the protein and fluorescent protein label.) The spliced fragments were then cloned into the vector pEXG2 [41]. Either mCherry or superfolder-GFP (sfGFP) was cloned into the BamHI site to construct a C-terminal fluorescent fusion to the target genes *clpV*, *tssB*, and *fha*. Finally, each fused gene was inserted at the endogenous promoters by allelic exchange, as described in Ref. [41].

An in-frame deletion of *retS* was introduced to the ClpV-mCherry/TssB-sfGFP strain using allelic exchange as described in [46].

Bacterial cultivation for strain construction was performed in Luria broth (LB) medium supplemented with 25 g/ml irgasan, 30 g/ml gentamycin, and counter selection for allelic exchange was performed on low-salt LB supplemented with 5% wt/vol sucrose.

2.5.2 Behavior of ClpV-TssB double fusion

The ClpV-mCherry/TssB-GFP double fusion measurably changed ClpV behavior compared to the ClpV-mCherry fusion alone. Although the single-label ClpV-mCherry focus lifetime is identical in both wild type and Δ*retS*, the ClpV-mCherry/TssB-GFP foci lifetimes are 10% longer in Δ*retS* where T6SS is over-expressed. Additionally, in wild type, the ClpV-mCherry/TssB-GFP strain has a diminished firing rate compared to the ClpV-mCherry fusion alone, with at most one ClpV spike seen over the 7–9 minute experiment with a spike lifetime five times as long as wild type ClpV-mCherry. Although this ob-

servation of less active dynamics might suggest loss-of-function, we performed a competition between *B. thailandensis* and the double-labeled wild type and the double-labeled and wild type cells had statistically indistinguishable fitness. We therefore believe that the qualitative localization dynamics observed in ClpV-mCherry/TssB-GFP Δ*retS* is informative, despite the failure of TssB-GFP to completely complement TssB with respect to the ClpV dynamics.

Supplemental figures

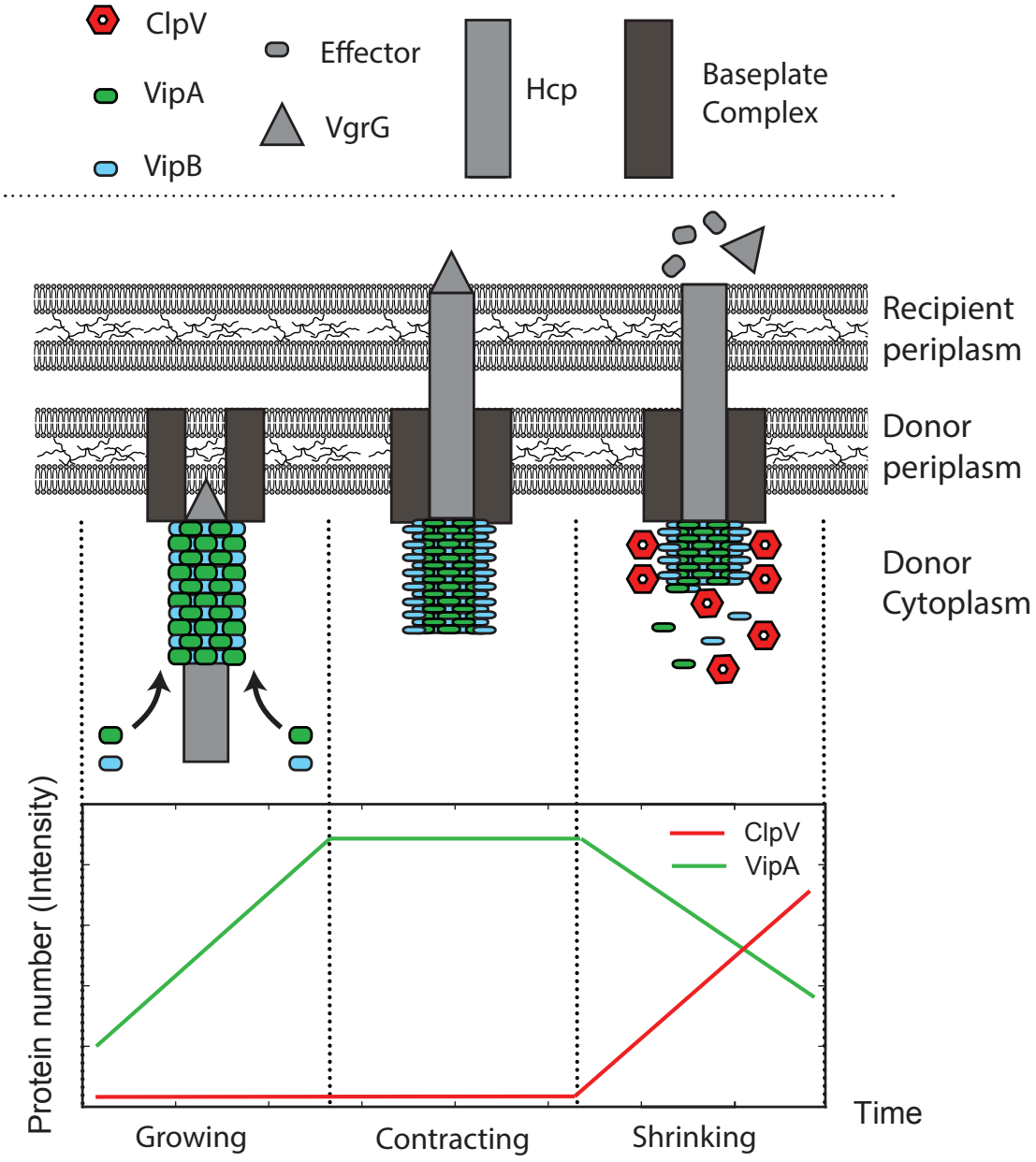

Figure 2.1: **Simplified schematic model for *V. cholerae* T6SS structure and secretion mechanism.** In *V. cholerae*, contraction of the TssBC sheath pushes the Hcp/VgrG needle through the recipient cell membrane. After this contraction, the N-terminus of TssC is exposed. Only then is ClpV attracted to the sheath, allowing ClpV to bind to TssC and disassemble the sheath.

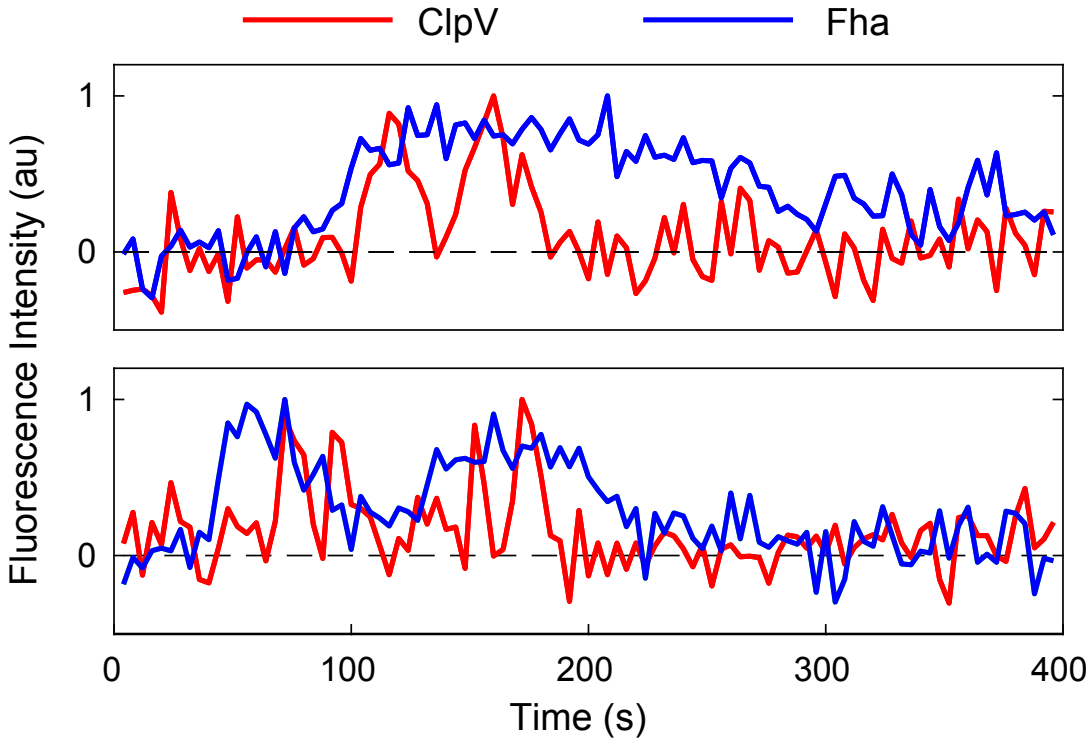

Figure 2.4: Representative intensity traces of ClpV and Fha. Top: Fha levels start increasing a few seconds before ClpV begins to fire. After the firing has terminated, Fha returns to a baseline level. Bottom: Fha disappears and returns. Due to the diffuse nature of the Fha focus, an automated approach was not reliable. The intensity traces shown above were representative of the $n \approx 1760$ traces examined by eye.

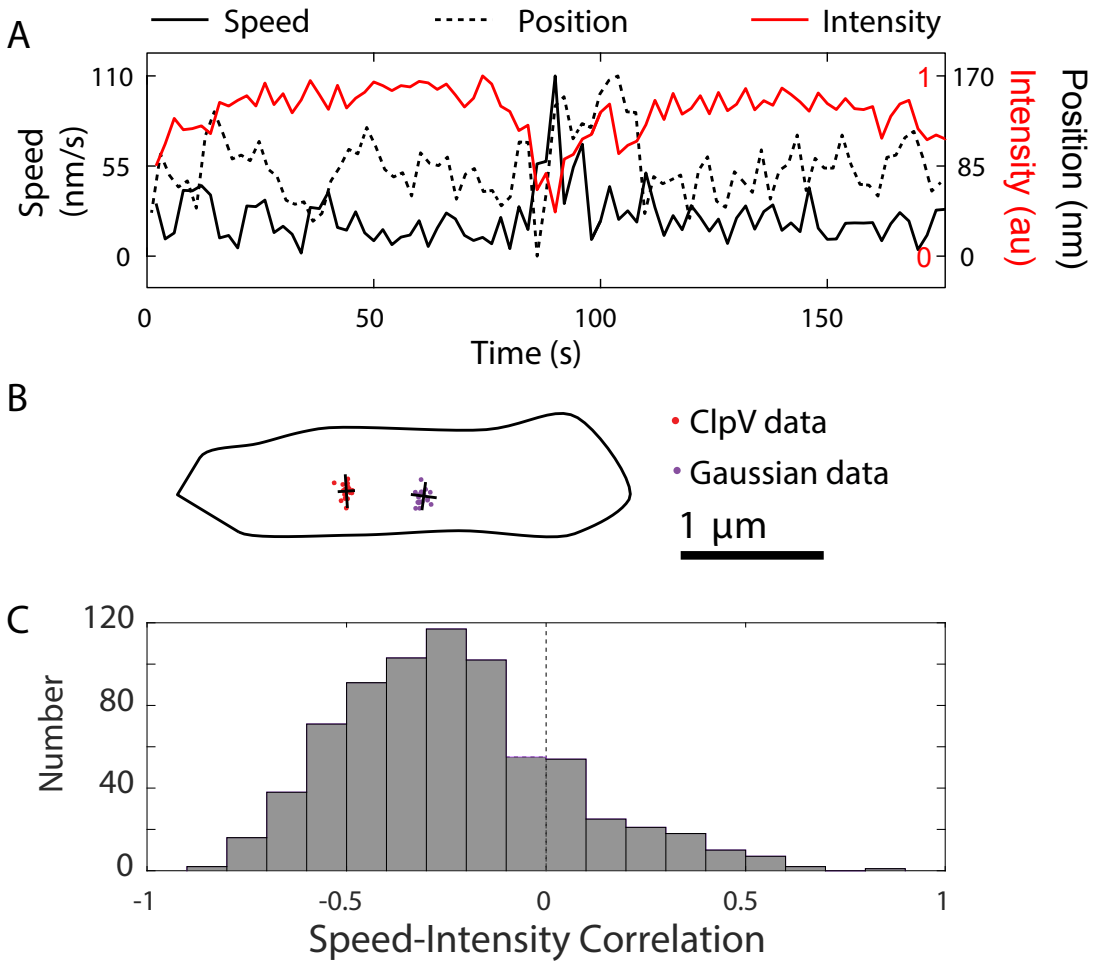

Figure 2.5: A: Example spread of ClpV data and Gaussian-distributed data. Major and minor axes are indicated in black. B: Representative intensity/position/speed graph for one region. Frame rate = 2 s. Position is measured by projecting coordinates onto best-fit line. C: Correlation coefficients between speed and intensity in wild type cells. $n \approx 650$. Typically there is a negative correlation between speed and intensity.

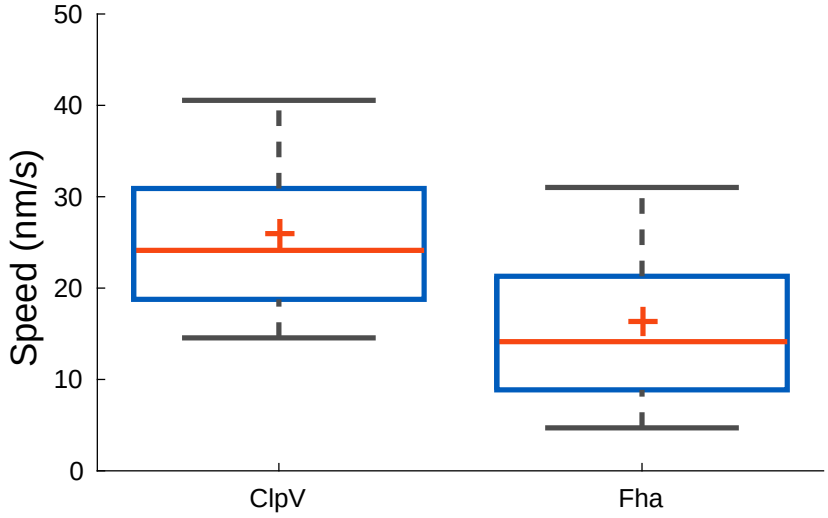

Figure 2.6: Box plot showing relative ClpV and Fha speeds. ClpV on average moves with greater speed than Fha, which is membrane-bound.

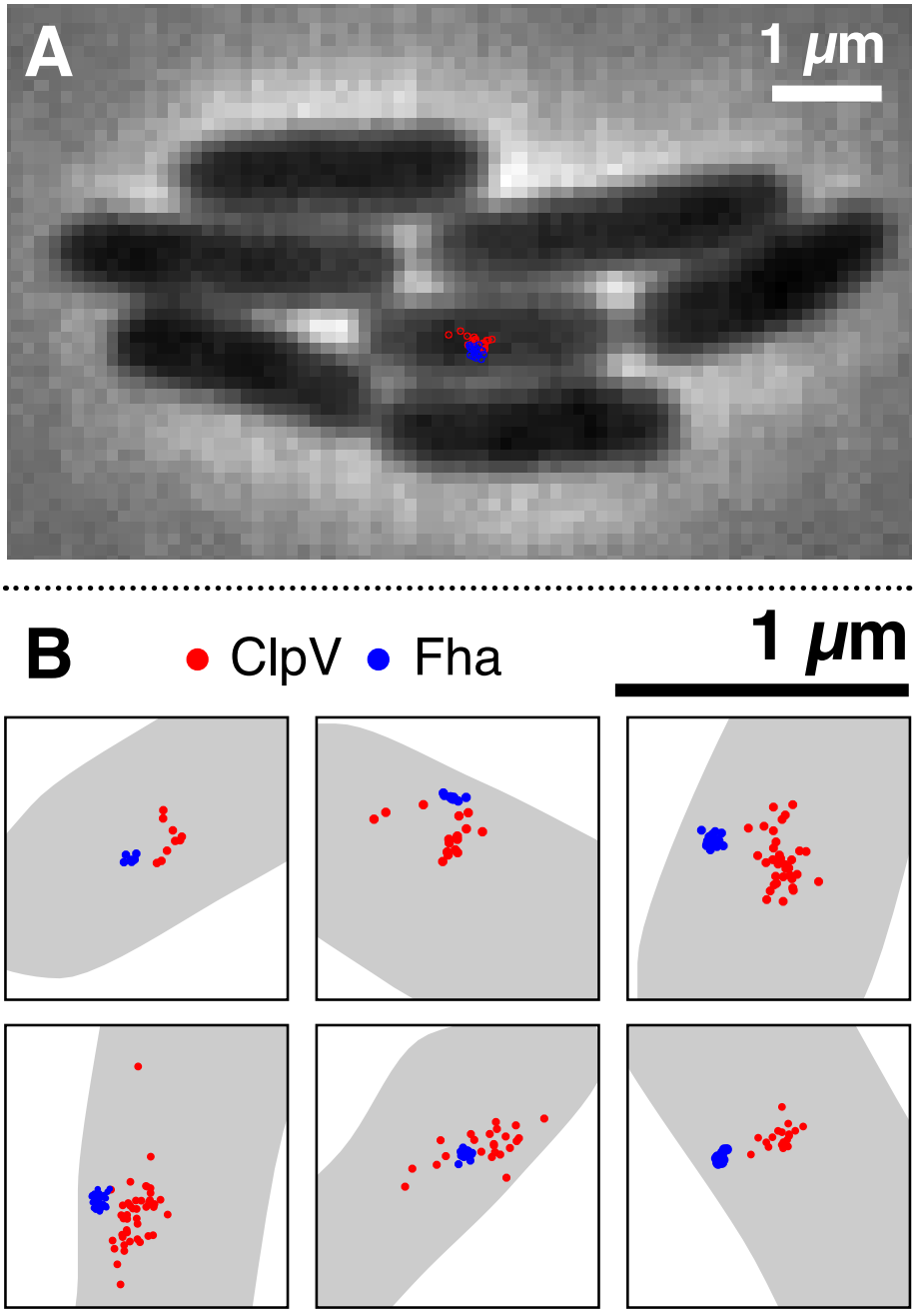

Figure 2.7: A: Brightfield image of cells with ClpV, Fha foci locations indicated. B: Representative ClpV, Fha distributions. Of note, while Fha is more tightly clustered, we do not always observe it on the long edge of the cell, and we do not always observe ClpV moving perpendicularly to the cell membrane.

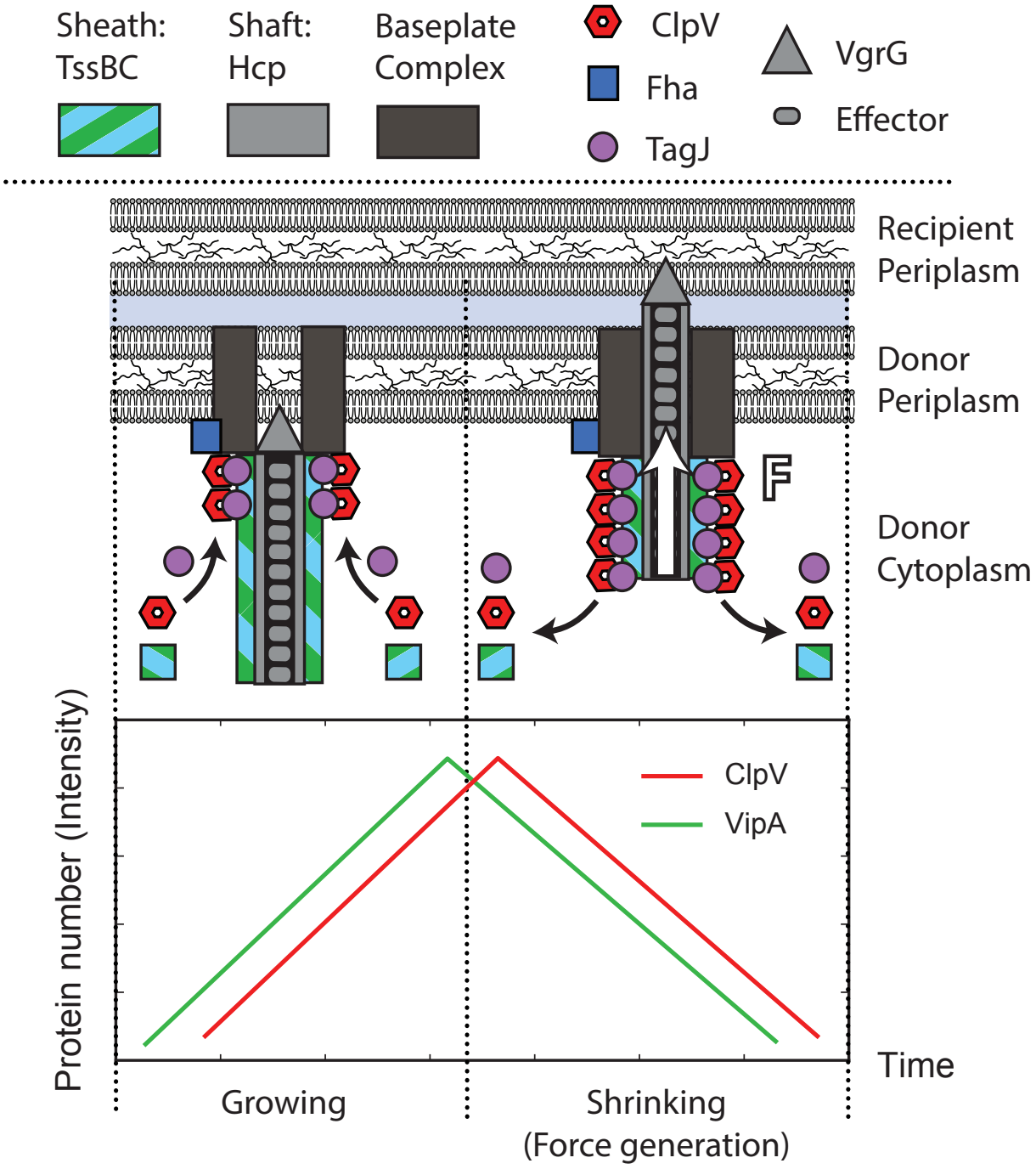

Figure 2.8: **Schematic model for *P. aeruginosa* T6SS structure and secretion mechanism.** Fha in blue; TagJ in purple; TssBC in green/blue; ClpV in red. Fha is a key component of the baseplate complex. TssB is an essential component of the sheath. TagJ allows ClpV to bind to TssB without any conformational change. As the TssBC sheath extends, ClpV disassembles the sheath, generating a force which pushes the Hcp/VgrG needle through the recipient cell membrane.

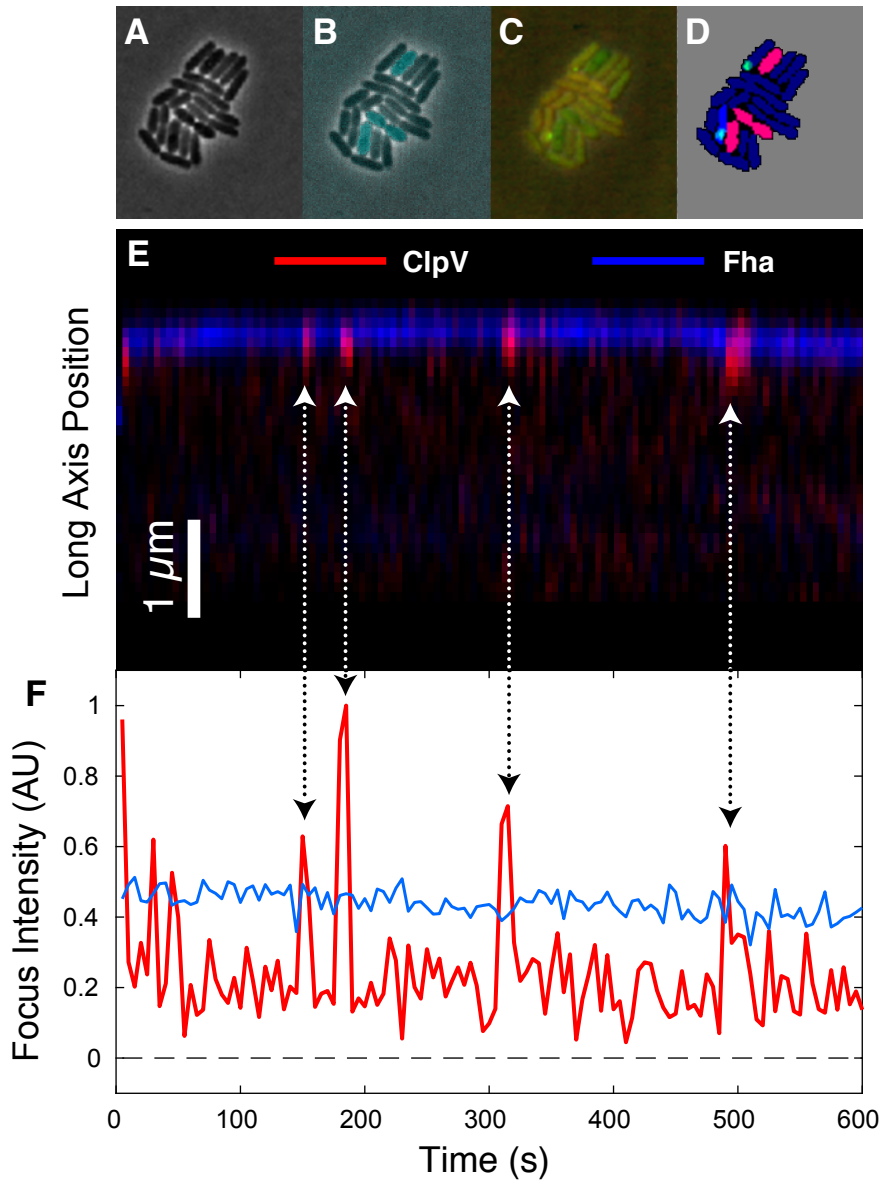

Figure 2.9: **Panel A:** Phase contrast image of polymicrobial microcolony consisting of both *P. aeruginosa* and *B. thailandensis* cells. **Panel B:** Cell identity is inferred by cytoplasmic fluorescence of CFP expressed in *B. thailandensis* cells. **Panel C:** ClpV-mCherry and Fha-GFP visualized by fluorescence microscopy in a single frame. **Panel D:** Cells are segmented from the phase contrast image, cell identity is inferred from CFP fluorescence and foci are detected in mCherry and GFP channels. *B. thailandensis* and *P. aeruginosa* cells are pink and blue respectively. Foci with (without) neighboring *B. thailandensis*are green (blue). **Panel E:** Kymograph showing fluorescence intensity of Fha (blue) and ClpV (red) long axis dynamics over a 4 minute interval. **Panel F:** Fha (blue) and ClpV (red) focus intensity dynamics. Arrows show the corresponding events in the kymograph and intensity plots.

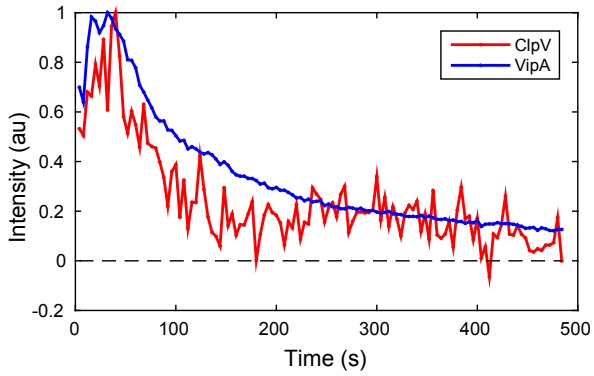

Figure 2.10: Example TssB/ClpV intensity trace in wild type. Key features include lack of repeated firing and unusually long firing lifetime, indicating that adding the TssB label restricts both ClpV and TssB firing activity.

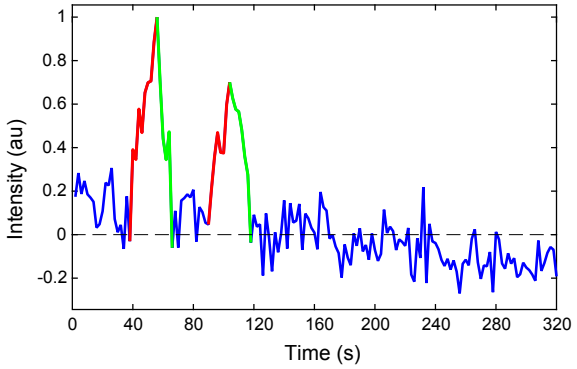

Figure 2.11: Visual example of our spike identification algorithm. We gated for spikes based on slope, relative intensity levels, and duration of activity. Red and green signify the two-part gating measure; each spike must have a beginning (red) and an end (green) to be recorded and measured.

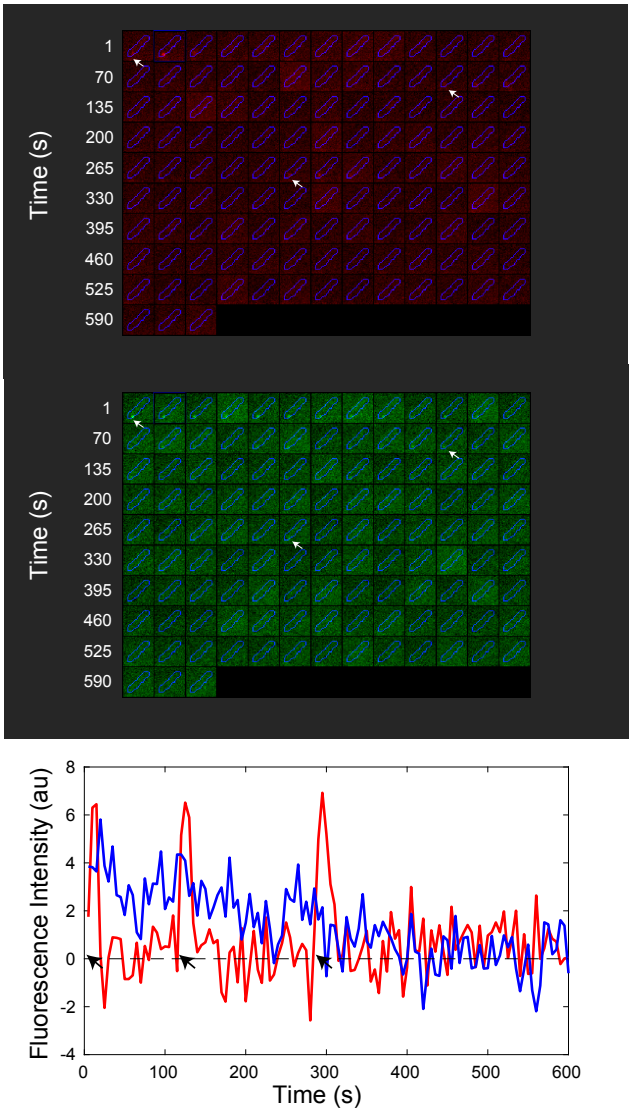

Figure 2.12: **Top:** ClpV foci over time. Arrows indicate the initiation of ClpV spikes. **Middle:** GFP foci over time. Arrows show Fha foci at time of ClpV spikes. **Bottom:** ClpV and Fha foci intensity trace over time. Arrows correspond with initiation of ClpV spikes and arrows in the upper frames.

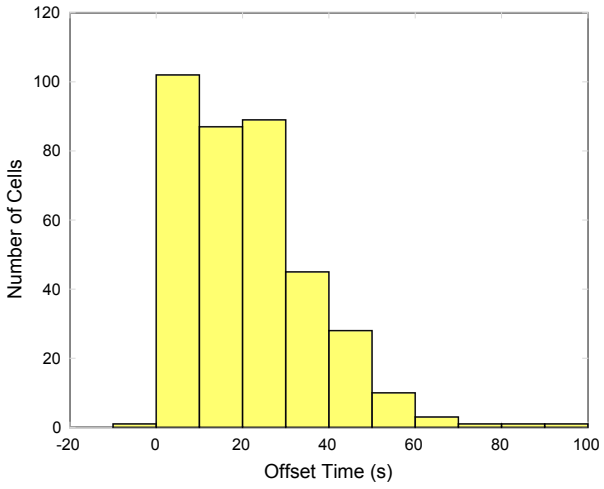

Figure 2.13: Number of seconds Fha appears before ClpV. Due to low signal-to-noise and varying Fha intensity growth patterns, making it difficult to consistently detect Fha appearance computationally, lag times were estimated individually. Fha appeared before ClpV in all but one cell. $n \approx 350$.

Chapter 3

T6SS ACTIVATION PATHWAYS IMPACT FUNCTION AND NEIGHBOR TARGETING IN *Pseudomonas aeruginosa*

3.1 Abstract

The Type Six Secretion System (T6SS) is a key determinant of bacterial fitness in polymicrobial communities. The secretion system functions as effector-delivery system which targets neighboring bacterial cells using a contact-mediated mechanism. Although much is known about the mechanism of the *V. cholerae* T6SS, there appears to be significant differences, even in the essential genes, between the *V. cholerae* T6SS and the T6SSs in other Gram-negative bacteria. In this paper we perform quantitative analysis of the function and dynamics of the H1-T6SS in *P. aeruginosa*. We present a detailed characterization of the T6SS visualized in single cells using quantitative image analysis of the dynamic localization multiple fluorescent fusions to T6SS proteins. We measure the rates of assembly and disassembly in wild type and mutants that affect T6SS activation and compare propensity to directly target competitor cells. Activation mechanisms prove to play a large role in both behavior and targeting of the *P. aeruginosa* H1-T6SS.

3.2 Introduction

Bacteria frequently need to compete against neighbors for resources including nutrients and habitat. Many bacteria have consequently developed defensive mechanisms to protect and advance their own territory. One prevalent mechanism is the Type Six Secretion System (T6SS), found in ≈25% of Gram-negative bacteria, including *P. aeruginosa* and *V. cholerae*. This system delivers toxic effectors to surrounding bacteria, causing lysis or cessation of growth [41]. It is known that this pathway requires cell contact to be effective

[27, 36]. However it is not well-understood how or even if these cells can sense contact by neighboring cells. Some species constitutively activate T6SS to respond to any threats proactively, and it is hypothesized that no sensing mechanism is required in this case. *P. aeruginosa*, on the other hand, has a non-constitutively activated mechanism, and a tit-for-tat mechanism has been proposed wherein the Hcp Secretion Island 1-encoded T6SS (H1-T6SS) in *P. aeruginosa* responds to a puncture in the cell membrane [8]. Additionally, in [cite], Δ*retS P. aeruginosa* has been shown to kill T6SS+ competitors above T6SS- competitors, and Δ*retS P. aeruginosa* is also more likely to kill T4SS+ competitors above T4SS- neighbors [cite].However, this mechanism has been observed but not quantified in the Δ*retS* background, and observed to not exist in the Δ*retS pppA* background.

There are also several known errors in the literature about H1-T6SS targeting. For example, initial analysis suggested that *P. aeruginosa* cells were more likely to form H1-T6SS foci if their neighbors also had H1-T6SS foci, but an error was found in this analysis [40], [Mougous lab, unpublished]. Additionally, the proposed mechanism for targeting is that the TagQRST/PpkA signal cascade senses membrane disruption, phosphorylates Fha1, and responds directly at the point of attack [8]. However, no H1-T6SS activation pathways are known to depend on neighboring cells, and the increased H1-T6SS activation could be explained through PARA, which activates H1-T6SS by responding to sister cell lysate. There is also not strong evidence that the TagQRST pathway is responsible for sensing an attack, as the evidence for that relied on observing H1-T6SS foci in a Δ*tagT retS* background but later experiments demonstrated that *tagT* is an essential H1-T6SS protein and its deletion prevents H1-T6SS assembly [8, 41].

Given that genetic modifications which impact T6SS activation can affect targeting behavior, and that targeting behavior has been mischaracterized in key ways in the literature, we chose to investigate functional differences in protein dynamics as well as targeting under four different activation conditions described below.

One activation pathway is posttranslational regulation by the threonine phosphorylation pathway (TPP). In this pathway, a fork head-associated domain-containing protein,

Fha1, is phosphorylated and precipitates further T6SS assembly and effector secretion [47]. A phosphatase, PppA, counteracts the phosphorylation of Fha1 by PpkA, restoring the system to its inactive state. Two impetuses are thought to trigger the TPP: surface-associated growth and membrane perturbation [64, 8]. This pathway can be activated by the deletion of the repressor protein, *pppA*. A more recently characterized pathway is *P. aeruginosa* response to antagonism (PARA). Described most thoroughly in Leroux *et al.*, H1-T6SS is activated in *P. aeruginosa* when *P. aeruginosa* is exposed to lysed *P. aeruginosa* cells [41]. Interestingly, given that a likely cause of lysed *P. aeruginosa* cells is non-self bacteria, the activation of PARA in any individual cell is independent of that cell neighboring any non-self cell. LeRoux *et al.* also demonstrated that PARA does not require the TPP, and instead works through the global activation of antibiotic and cyanide synthesis/regulator of secondary metabolism (Gac/Rsm) pathway [41]. The Gac/Rsm pathway is a global regulatory system which affects production of proteins through RsmA, a CsrA-type protein which predominantly represses translation of target mRNA molecules to which it binds [39]. PARA also co-occurs with changes in T6SS gene expression, further indicative that this pathway is separate from the TPP, a posttranslational regulator of H1-T6SS [41]. This pathway is also activated through the deletion of *retS*, in this study considered a separate method of H1-T6SS activation. A third independent activation pathway is less understood. TagF is a posttranslational repressor of the H1-T6SS, and while shown to be independent of TPP and PARA, has very little else characterized [41]. This pathway can be activated through the deletion of *tagF*.

While the methods of activation pathways of H1-T6SS in *P. aeruginosa* remain a subject of thorough investigation, characterizing dynamic changes in H1-T6SS behavior as a function of activation pathway has remained relatively untouched, and targeting differences between these strains are not well quantified. Here, we investigate dynamic differences in three essential components of the H1-T6SS Fha, TssB, and ClpV - in strains in *P. aeruginosa* activated in each of these four ways, improving our understanding of the function of each of these pathways.

3.3 Results

3.3.1 ClpV dynamics depends on activation pathway.

Unlike *V. cholerae* which is constitutively active, the H1-T6SS must be activated in *P. aeruginosa*. The functional consequences of this regulation on ClpV dynamics have not yet been investigated. We hypothesized that ClpV localization dynamics could be highly dependent on the activation mechanism. We therefore constructed ClpV-sfGFP and ClpV-mCherry fusions in three contexts where T6SS is activated: wild type activated with PARA, Δ*pppA* and Δ*tagF*. We then performed a quantitative analysis of the localization dynamics in each background.

Both the quantitative and qualitative nature of this firing pattern was background-dependent. In strains activated via Δ*pppA* and Δ*tagF* deletion, ClpV spikes did not form clear groupings since the pause time had a significant increase in duration and variance (Fig. 3.1). The mean pause times including both grouped and ungrouped spikes were 25 s, 40 s and 52 s for PARA, Δ*pppA* and Δ*tagF* respectively. In spite of the increased pause time, the T6SS Fha focus remained stationary in the cell.

3.3.2 Fha dynamics depends on activation pathway.

Fha persists indefinitely in pppA and tagF. Because phosphorylation of Fha is required in the TPP but not under PARA or Δ*tagF* activation, we were particularly curious if this difference in phosphorylation requirement impacted Fha dynamics across the different genetic backgrounds [47]. In the Δ*pppA* background, we observed that the stability of the Fha focus significantly increases. The Fha focus rarely disappears over the time scale of the experiment (7-9 minutes) (Fig. 3.2). This observation is consistent with the known functional phenotype of Δ*pppA*, the activation of T6SS. These observations are consistent with the phosphorylation of Fha directly determining the complex lifetime. Next we investigated the Δ*tagF* background. Since TagF does not activate the T6SS by the phosphorylation of Fha, it was not obvious how the tagF mutant would affect Fha localization. To

our surprise, the tagF phenotype was essentially identical to the pppA phenotype, stabilizing Fha focus intensity, but without directly affecting the phosphorylation of Fha since the activation via the tagF pathway is independent of p-Fha [64].

3.3.3 ClpV dynamics does not depend on cell contact.

A number of mechanisms of T6SS assembly have been proposed that depend on cell contact. For instance, Basler *et al.* have shown that local membrane perturbations activate T6SS and have proposed a tit-for-tat activation mechanism in which a cell targeted by T6SS, assembles its own T6SS at the location of the attack to respond [8]. We therefore hypothesized that ClpV dynamics in *P. aeruginosa* should depend on cell contact. However, there was little to no distinction in ClpV behavior with or without contact with *B. thailandensis* (Fig. 3.3).

3.3.4 T6SS is not more active in cells neighboring B. thailandensis

T6SS effectiveness is dependent on direct delivery of toxins to neighboring cells, so we hypothesized that it would be beneficial for H1-T6SS in *P. aeruginosa* cells to target non-self neighbors. First, we determined whether H1-T6SS foci are more likely to appear if they are neighboring a competitor cell (in this case, *B. thailandensis*) or neighboring a sister cell. We hypothesized that if targeting occurred, it would be advantageous for H1-T6SS foci to preferentially activate when near competitor cells rather than when near sister cells. Additionally, since *B. thailandensis* has a T6SS which is constitutively active under lab conditions, we would also expect that if membrane perturbation triggered H1-T6SS activity that *P. aeruginosa* cells neighboring *B. thailandensis* would have increased H1-T6SS foci. However, Fig. 3.4**top**, showing H1-T6SS formation rates of wild-type cells activated via PARA, is inconsistent with this hypothesis. H1-T6SS foci formation is not dramatically impacted by having one or more neighbor cells, indicated here by percentage of cell membrane in contact with a neighbor cell, and the rate of foci formation appears to be con-

sistent whether the *P. aeruginosa* cell is neighboring *B. thailandensis* or a sister *P. aeruginosa* cell. The one exception to this trend is the comparison between having no *B. thailandensis* neighbors and having no *P. aeruginosa* neighbors - activity is actually slightly increased when no *B. thailandensis* neighbors are present compared to when no *P. aeruginosa* neighbors are present. This observation which is in direct contrast to our initial hypothesis.

This same behavior is observed in the pppA and tagF deletions, indicating that neither the TPP nor the tagF activation pathway is activated by cell-cell contact.

3.3.5 H1-T6SS foci localization to neighbors

Historically, targeting has been measured in two ways: through competition and through fluorescence microscopy of T6SS foci. Interestingly, although qualitatively ClpV foci in *P. aeruginosa* were observed to localize to *V. cholerae*, there was no quantification of this measurement nor a comparison to whether this measurement was above random [8]. We therefore first investigated whether T6SS foci localized closer to competitors and then compared this observation to random. We thus tested whether H1-T6SS could identify and localize to non-self neighbors above random under each of the above activation conditions. We investigated the interactions between WT, pppA, and tagF strains in *P. aeruginosa* and *B. thailandensis*, a known competitor species with its own T6SS apparatus. In interest of determining whether foci localized toward the side of the membrane which neighbored *B. thailandensis*, we compared a model of foci distributed randomly to our measurement of foci localizing toward the *B. thailandensis* membrane. In experiment, we tracked ClpV1-mCherry/Fha1-sfGFP fusions over time. Since these proteins colocalize, the focus regions are the same for both proteins. We determined the brightest location within the focus region, indicating the focus centroid, and determined whether the focus was neighboring a competitor cell, a sister cell, or no cell at all. We then generated randomly distributed foci within each of the cells and calculated the probability of the focus neighboring each of these options. For our simulation, we identified all cells within

each strain that had both a *B. thailandensis* neighbor and a T6SS focus, wrote a simulation which randomly generated foci within each of these cells, and determined whether each focus localized toward *B. thailandensis* or not. We repeated the simulation 10 times in each cell, and calculated the population average for each strain. Results are in Fig. 3.5. Foci are about as likely to border *B. thailandensis* cells as would be expected by random, but interestingly are slightly more likely to border sister cells than would be expected by random in all cases except the Δ*retS* background. We hypothesized that this behavior could be explained by the behavior observed in Vettiger *et al.*, where H1-T6SS substrates are exchanged between *P. aeruginosa* cells [72]. Perhaps an H1-T6SS attack from a neighboring *P. aeruginosa* cell delivered extra substrates near the donor *P. aeruginosa* cell, supporting H1-T6SS foci formation near the donor cell. In this model, if a donor cell had a focus, the recipient cell would soon form a focus near the location of the original attack, exhibiting previously observed tit-for-tat behavior [8, 40].

3.3.6 Tit-for-tat behavior only observed in ΔretS background

To investigate the model suggested by our previous experiment, we investigated tit-for-tat behavior in all four activation methods. To quantitatively characterize tit-for-tat behavior in a manner unprecedented in current literature, we compared measurements of tit-for-tat behavior to simulations of randomly distributed foci in the same cells, described below, to ensure that the measured tit-for-tat behavior was above random. We anticipated that we would not see tit-for-tat behavior in Δ*pppA* nor Δ*tagF* backgrounds because the foci were stationary and so unable to respond to new threats. We used these backgrounds as controls. We anticipated seeing tit-for-tat behavior in both Δ*retS* and wild-type backgrounds.

Because a response to an attack could appear after the original focus had disassembled, we removed all temporal information from the foci and looked at all foci which appeared over the timelapse. We did this by identifying all foci regions as described in

Materials and Methods and plotting all these foci regions simultaneously on the cell identification image (the full version of Fig. 3.6E). Tit-for-tat behavior was then determined as described in Fig. 3.7.

Since the rate of H1-T6SS activation is different between these activation methods (as discussed in section 1.3.3), we compared the measured tit-for-tat behavior to simulation of random foci for each strain. We ran two types of simulations, one simulating a new randomly positioned focus in each cell and comparing foci matching to the other actual foci surrounding it (referred to in Table 3.1 as "Simulate-one"), and a simulation where all foci in the data set were randomly repositioned within their cell and foci matching was measured (referred to in Table 3.1 as "Simulate-all". A demonstration of this is shown in Fig. 3.7. Results can be seen in Table 3.1.

The percentage of foci matching varied between strains, at least partially dependent on the rate of activation and the concentration of *P. aeruginosa* on the slide. For instance, wild type has a particularly low percentage of measured foci matching since in this strain H1-T6SS was activated using PARA, requiring *B. thailandensis* presence on the slide, and in this experiment, foci matching was measured only between *P. aeruginosa* cells. Thus, the relevant information comes from the z-scores of each simulation, comparing the measured foci matching to that of the same number of foci.

Interestingly, Simulate-one had z-scores that were usually about twice as high as those for Simulate-all. However, the specific z-score is not as important as the comparison to the z-scores of Δ*pppA* and Δ*tagF* backgrounds, our controls for no targeting response. The z-scores in these backgrounds ranged about 2-4. In comparison, wild type also had z-scores in this range, while Δ*retS* had z-scores well above this range. In this comparison to simulation, we thus see that the previous studies of foci matching in the Δ*retS* background are describing real behavior. However, the true surprise comes from the wild type background, where foci matching is not above our controls, suggesting that targeting is specific to the Δ*retS* background.

Table 3.1: Simulation Results for foci matching in four genetic backgrounds. Z-score is given for measured targeting compared to the simulated targeting in each case.

Simulation Type	Δ*retS*	wild type	Δ*pppA*	Δ*tagF*
Measured targeting	27.4	5.4	12.6	9.4
Simulate-one (z-score)	19.1 (14.5)	4.0 (3.3)	8.9 (2.9)	6.9 (4.2)
Simulate-all (z-score)	18.7 (7.9)	4.4 (1.4)	10.3 (2.3)	7.3 (1.9)

3.3.7 Foci matching in the ΔretS background has a clearly defined response time

To confirm that our observed foci matching represented real behavior, we measured the time for one focus to appear in response to another focus. This was important to eliminate the possibility that the measured foci matching included foci that appeared minutes after the initial attack and are thus less likely to have appeared in response to an attack. To measure foci response time, we recorded the time difference between when one focus appeared and its matching focus appeared.

To make this measurement, we did not include foci matching pairs where one or both of the foci were present in the first frame of the timelapse, since it would be impossible to measure when the first focus appeared. Additionally, foci matching was initially measured using a ClpV-mCherry/Fha-sfGFP fusion, and foci were counted if an Fha focus was present even if ClpV firing was not observed in that timelapse. This measurement clearly required a ClpV spike to appear in the timelapse, and so foci matching pairs where in one or more foci only Fha was present were not included either. Finally, we knew that the response time should be on the order of seconds, not minutes, so we only investigated the first four minutes of each timelapse to eliminate non-biologically-relevant foci matching.

These three restrictions significantly impacted the number of foci matching events we were able to observe in each of the four genetic backgrounds. See Fig. 3.8 for results.

The clear foci response time of 15 s in the Δ*retS* background provides further evidence

that the tit-for-tat behavior characterized in this background is a real phenomenon. It is interesting to note, however, that again the wild type background does not show obvious signs of imitating Δ*retS* behavior with a peak at 15 s.

3.4 Discussion

3.4.1 ClpV and Fha dynamics depend on activation pathway but not cell contact

While in cells where H1-T6SS is activated via the Gac/Rsm pathway (both wild type and Δ*retS*) Fha both appears and disappears on the order of minutes, in both the Δ*pppA* and Δ*tagF* backgrounds Fha persists through the length of the time lapse without significant intensity decrease. This is unsurprising for the Δ*pppA* background, since the deletion of *pppA* activates H1-T6SS by abrogating the ability to dephosphorylate Fha, and thus we expect persistent Fha foci [64, 8]. The pathway which relies on *tagF*, however, is not well understood, and like the Gac/Rsm pathway is known to not rely on p-Fha [64]. These observations suggest that the *tagF* pathway depends on regulation of Fha, providing more evidence that Fha is a key regulatory protein of H1-T6SS.

ClpV dynamics also varied with activation pathway, but this variance appeared to depend on Fha localization. Characterization of over 3000 cells in all activation pathways show that ClpV spikes never occur without Fha presence, and observation of over 1000 cells in the Δ*pppA* and Δ*tagF* backgrounds show that ClpV often continues to fire intermittently while Fha is present, explaining the increased time between ClpV spikes in these backgrounds (Fig. 3.1). Given that no other ClpV behavior changes measurably in these different backgrounds nor by contact with cells, it seems reasonable to hypothesize that the ClpV firing is regulated by Fha presence, and therefore that if Fha is present, H1-T6SS fires at a rate dependent on protein synthesis.

3.4.2 *H1-T6SS foci formation does not depend on neighbors under any activation condition*

In contrast to earlier published papers, we determined that H1-T6SS is not more likely to form when it neighbors cells which also have foci. We also determined that foci are not more likely next to form near *B. thailandensis* neighbors, but may be slightly more likely to form next to sister cells. This is in direct contrast to current published literature, which suggests that *P. aeruginosa* is more likely to form foci when its membrane has been disrupted [40, 29]. In contrast, we hypothesize that the rate of H1-T6SS formation is not dependent on subcellular recognition of membrane disruption, but rather on recognition of external factors such as sister cell lysate in PARA or quorum sensing at a cellular level [41, 57].

3.4.3 *The ΔretS background is the only genetic pathway which exhibits tit-for-tat behavior*

We expected both the Δ*retS* and wild type cells to exhibit tit-for-tat behavior. These two genetic backgrounds are activated using the same pathway and have the ability to respond to dynamic external behavior, in contrast to the Δ*pppA* and Δ*tagF* backgrounds, which both have persistent Fha foci and do not dynamically form H1-T6SS foci over the time lapse we investigated. Δ*retS* cells showed tit-for-tat behavior at a rate well above that expected by random and also had a response time to neighboring foci of about 15 s. However, wild type cells seemed to exhibit tit-for-tat behavior at roughly the same rate as random and also did not exhibit any definitive response time. This more closely matched the Δ*pppA* and Δ*tagF* backgrounds, used as controls for absence of tit-for-tat behavior.

This surprising result opens up many questions. It seems apparent that tit-for-tat behavior would be beneficial for the organism to target surrounding aggressors. However, the lack of increased H1-T6SS formation near the competing bacterial species *B. thailandensis* as well as the lack of tit-for-tat behavior in wild type *P. aeruginosa* suggests that wild type *P. aeruginosa* do not dynamically respond to threats under lab conditions. Future studies may investigate other conditions more representative of normal bacterial com-

munities to determine if tit-for-tat behavior is activated under wild type under different conditions than those used for single-cell microscopy. The Δ*retS* background may represent a state which wild type cells reach only under certain growth conditions, and so yet may be illustrative of wild type behavior in clinical settings. In any case, it is not obvious that the tit-for-tat behavior observed in Δ*retS* should be used as a proxy to describe wild type H1-T6SS behavior.

3.4.4 Conclusion

We report on several measurements of H1-T6SS under various activation conditions using quantitative image analysis of single cells. While many aspects of the H1-T6SS behavior are the same regardless of these activation conditions, the differences demonstrate that regulation of the T6SS is dependent on Fha, not on any type of interaction with surrounding cells, and that even the well-characterized tit-for-tat behavior in *P. aeruginosa* is not universal among all cells which can dynamically respond to their environment. These measurements suggest a converging point for regulation, at Fha, as well as subtleties in the genetic backgrounds which suggest that gene deletion for purpose of H1-T6SS activation may impact the function of H1-T6SS at a deeper level than previously hypothesized.

Methods

3.4.5 Strains

Strains used in this study are described in Tab. 3.2. Strains were derived from *P. aeruginosa* PAO1 and *B. thailandensis* E264 [67, 74]. Functional translational fluorescent C-terminal fusions of either superfolder GFP (sfGFP) or monomeric mCherry (mCherry) were generated to TssB, ClpV, and Fha at their endogenous chromosomal loci by allelic exchange, as described in the supplement [41].

Table 3.2: Strains used in this study

Organism	Genotype	Source
Pseudomonas aeruginosa PAO1	*clpV-GFP*	Mougous *et al.* 2006. Science. 312:1526-30.
	tssB-sfGFP clpV-mCherry	This study
	ΔretS tssB-sfGFP ClpV-mCherry	This study
	fha1-sfGFP clpV-mCherry	This study
	ΔpppA fha1-sfGFP clpV-mCherry	This study
	ΔtagF fha1-sfGFP clpV-mCherry	This study
Burkholderia thailandensis	*attTn7::Tp-CFP*	LeRoux *et al.* (2015) *eLife*

3.4.6 Growth conditions and microscopy

All strains were grown overnight from a single colony in Luria Broth (LB) media. Doubling time in liquid media was roughly 30 min. Overnights were diluted 1:10 into fresh media and grown to $OD_{600} \approx 0.8$. (T6SS is less active in log-phase growth [41].) Agarose pads were prepared by pouring 1 mL of growth media and 0.2% agarose into 2 cm $\times$ 2 cm wells cut into a rubber gasket sealed onto a standard microscope slide. We spotted 2 μL of cells onto dried pads and a cover slip was placed on top of the pad. The entire slide was sealed with VaLP (1:1:1 Vaseline, lanolin, paraffin).

To study interactions with a second species, we introduced *B. thailandensis*. *B. thailandensis* was distinguished from *P. aeruginosa* by expression cytoplasmic CFP and gating cells on fluorescence levels in the CFP channel. Introducing *B. thailandensis* also has the advantage of activating T6SS in wild type *P. aeruginosa* [41]. Under normal growth conditions, wild type *P. aeruginosa* has about 1-2% of cells with an active T6SS as identified by the presence of a ClpV focus, but upon exposure to *B. thailandensis*, which activates T6SS via '*P. aeruginosa* response to antagonism (PARA), about 10% of cells have a ClpV focus [41]. All wild type cells in this study were activated via PARA to achieve a higher percentage of cells with foci. To activate *P. aeruginosa* via PARA, immediately prior to spotting cells on the s we added 100 L *B. thailandensis* to 100 L *P. aeruginosa* and spun down (3 min 8000 rpm), removed the supernatant, and resuspended the pellet in 40 L fresh LB before spotting.

Under imaging conditions, the average doubling time for cells was $\approx$ 40 min. Fluorescence microscopy was performed on a Nikon-TiE (Nikon, Tokyo, Japan) with environmental chamber using NIS-Elements software. Images were captured on an Andor Neo sCMOS camera (Belfast, Northern Ireland) at either 2 s or 5 s intervals.

To ascertain the functionality of these strains, we performed bacterial growth competition experiments with fluorescently labeled and unlabeled strains with *B. thailandensis* recipients under comparable conditions. T6S-dependent fitness was determined by com-

paring the ratio of *P. aeruginosa* to *B. thailandensis* before and after 7 hours of co-culture. We found that all strains reduced populations of *B. thailandensis* in a T6S-dependent manner by at least one order of magnitude.

3.4.7 Quantitative image analysis

Cells were segmented and linked from phase contrast images using our *SuperSegger* segmentation engine [69]. All time-lapse images were aligned to compensate for stage drift. Cell growth was not appreciable over times-lapse experiments, as observed by phase contrast microscopy. Although SuperSegger can identify and track foci, the current implementation identifies foci in each frame and links foci between frames. This approach is problematic for foci that repeatedly appear and disappear, since it can be difficult to ascertain whether a focus is returning to precisely the same location or not. In the current context, foci are imaged over a sufficiently short period that the movement of foci in this system is small ($<$500 nm). We therefore exploited these slow dynamics to track foci which reappear over time. We first averaged over all frames to generate a summed image, then identified loci in this summed image and defined a circular region (radius 500 nm around the focus position) where loci are allowed to move. To compute the focus intensity in each frame, we convolve each image with a disk (radius 300 nm), and define the focus intensity as the maximum pixel value in the allowed region of the convolved image minus the background intensity. We compute the background intensity by averaging over the fluorescence intensity in the cell, having first masked out the focus using the 300 nm radius disk.

3.5 Supplemental Information (SI)

3.5.1 Strain construction

Fluorescent fusions to endogenous genes were constructed as follows: The 500 bp regions flanking the C-terminus (stop codon) of each target gene was amplified. These flanking

regions were spliced together using a BamHI site (GGTACC) replacing the stop codon of the target gene. (The BamHI sequence acted as a two residue linker between the protein and fluorescent protein label.) The spliced fragments were then cloned into the vector pEXG2 [41]. Either mCherry or superfolder-GFP (sfGFP) was cloned into the BamHI site to construct a C-terminal fluorescent fusion to the target genes *clpV*, *tssB*, and *fha*. Finally, each fused gene was inserted at the endogenous promoters by allelic exchange, as described in Ref. [41].

In-frame deletions of *retS*, *pppA*, and *tagF* were introduced to the ClpV-mCherry/TssB-sfGFP strain using allelic exchange as described in [46].

Bacterial cultivation for strain construction was performed in Luria broth (LB) medium supplemented with 25 g/ml irgasan, 30 g/ml gentamycin, and counter selection for allelic exchange was performed on low-salt LB supplemented with 5% wt/vol sucrose.

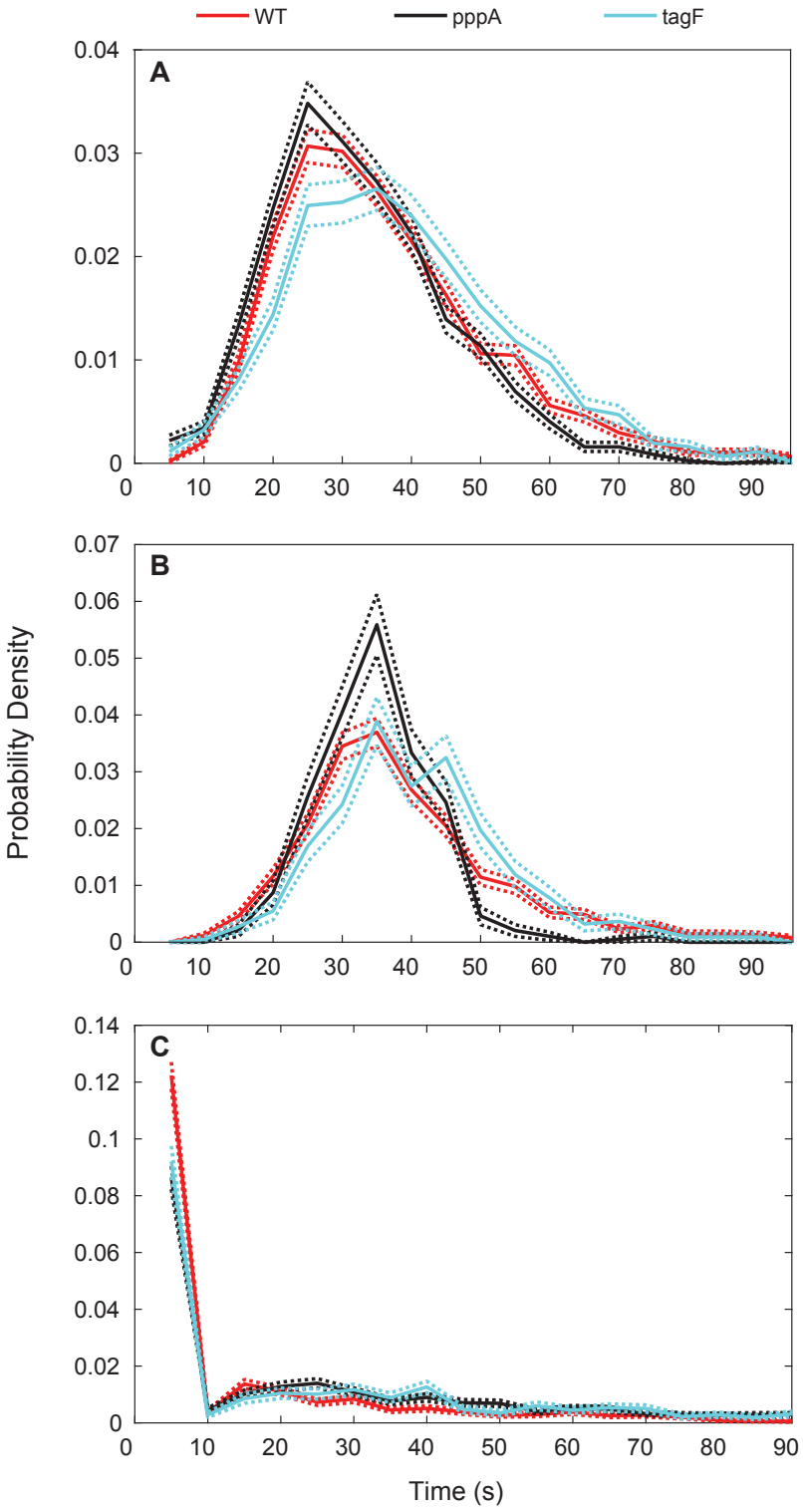

Figure 3.1: Data for each activation pathway is shown. **Panel A:** Average lifetime of each ClpV1 firing event. **Panel B:** Average lifetime of ClpV1 firing events per cell. **Panel C:** Spacing between ClpV1 firing events. Wild-type: $n \approx 1900$. Δ*pppA*: $n \approx 400$. Δ*tagF*: $n \approx 500$.

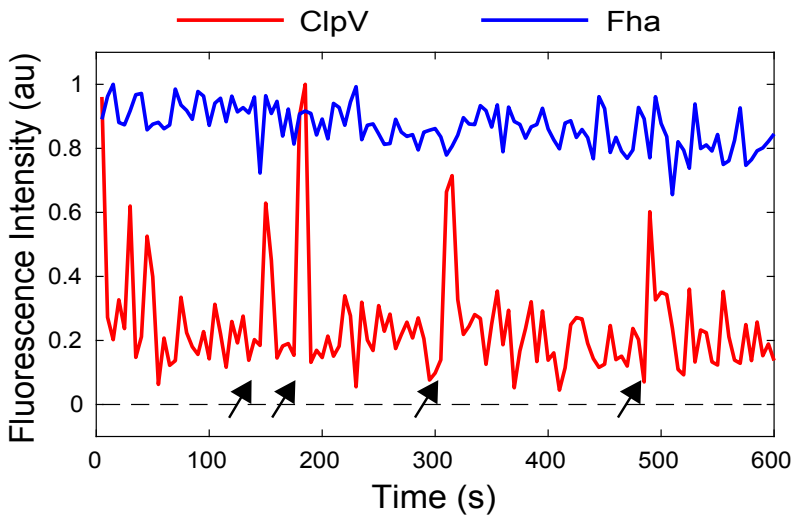

Figure 3.2: Example trace for consistent Fha lifetime. Arrows indicate firing events that continue to occur throughout the timelapse.

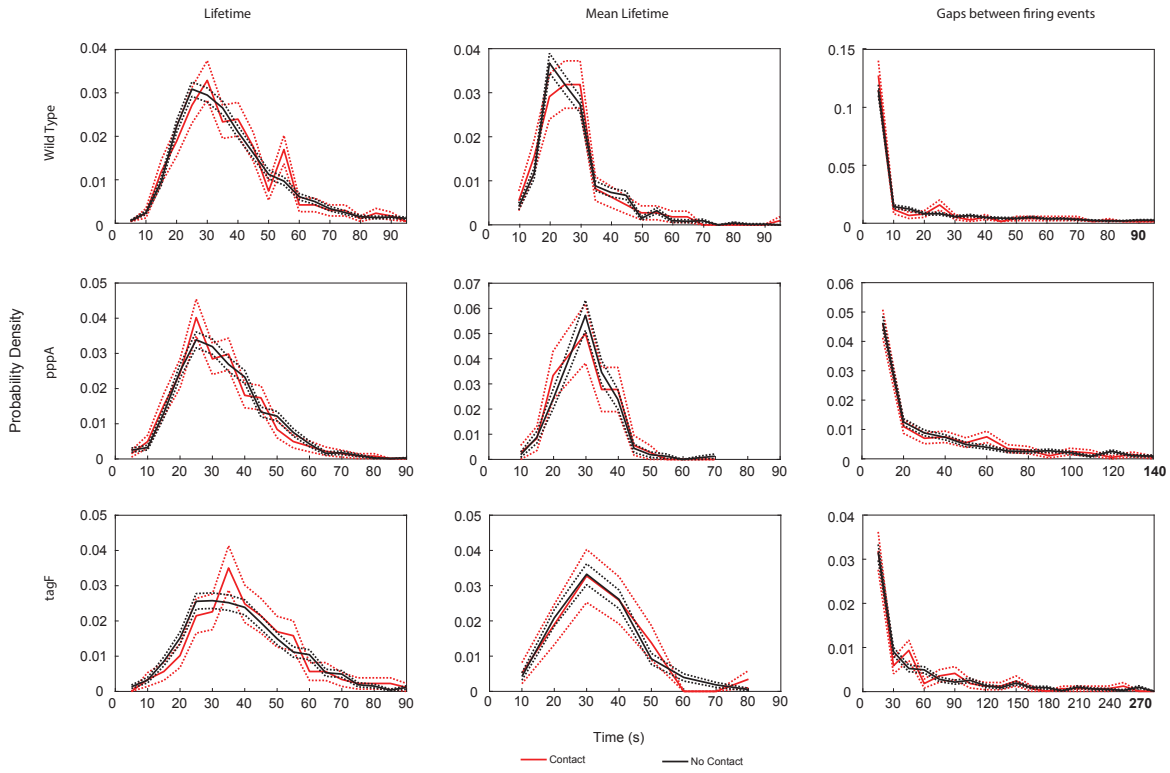

Figure 3.3: Data for each measurement and each activation pathway is shown grouped by contact or lack of contact with *B. thailandensis*. There appear to be no significant behavioral differences based on contact with *B. thailandensis*. Wild-type: $n \approx 1900$. Δ*pppA*: $n \approx 400$. Δ*tagF*: $n \approx 500$.

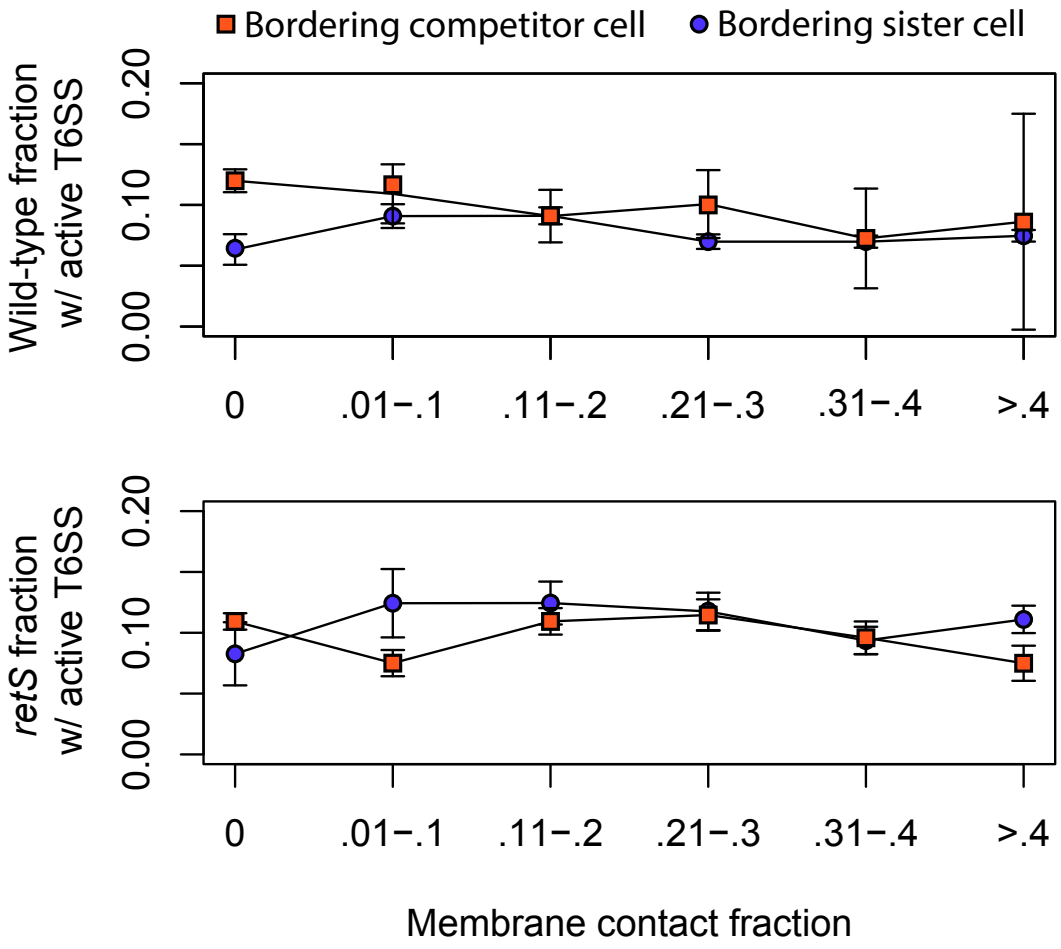

Figure 3.4: Fraction of cells with ClpV foci versus fraction of membrane contacting. **Top:** Wild-type. $n \approx 1900$. **Bottom:** $\Delta retS$. $n \approx 700$. There is no marked change in ClpV foci formation as contact with neighbor, either sister or competitor, increases.

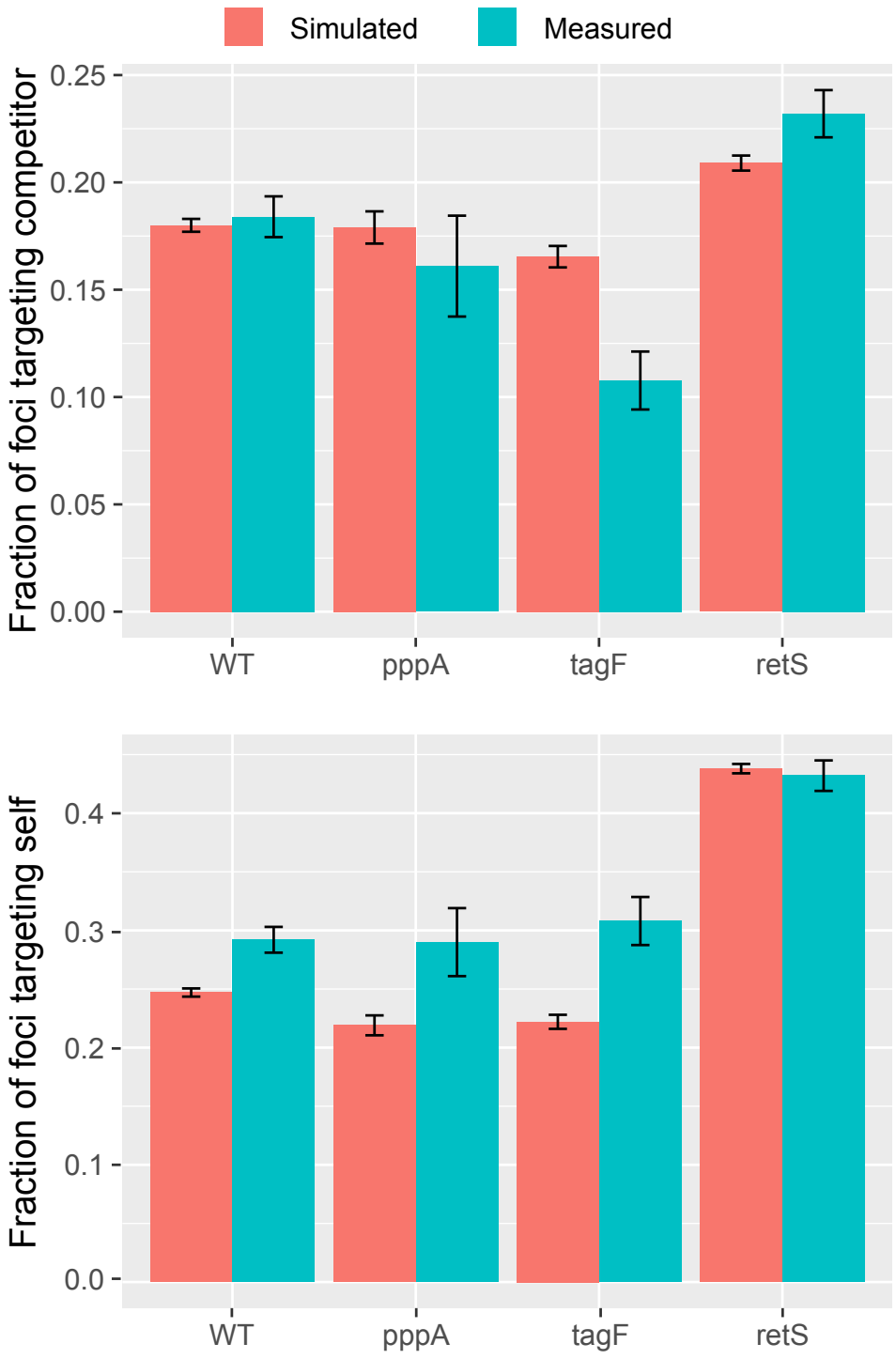

Figure 3.5: Comparison of simulation vs. actual (measured) localization of T6SS foci toward neighbor. **Top:** Simulated vs. actual measurements of H1-T6SS foci localizing near *B. thailandensis* neighbor. **Bottom:** Simulated vs. actual measurement of H1-T6SS foci localizing near *P. aeruginosa* neighbor. Wild-type: $n \approx 1900$. Δ*pppA*: $n \approx 400$. Δ*tagF*: $n \approx 500$. Δ*retS*: $n \approx 700$.

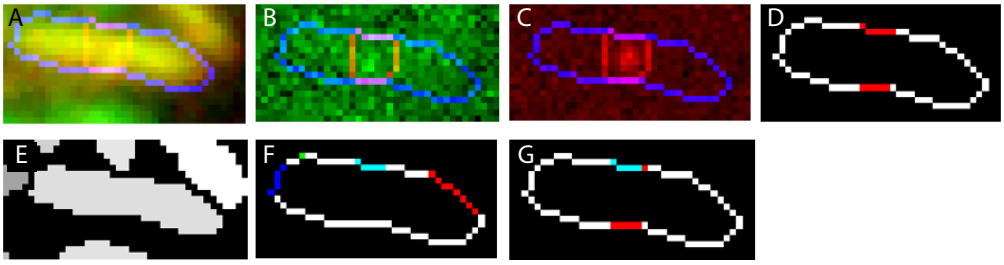

Figure 3.6: **A:** Summed image of both mCherry and GFP channels with the cell of current interest outlined in blue. *B. thailandensis* appears green because its cyan label is also visible in the GFP spectrum. *P. aeruginosa* appears yellow because it has both red and green fluorescence. **B:** One time stamp of the GFP channel to show the focus located in the region of interest. **C:** One time stamp of the mCherry channel to show the focus located in the region of interest. **D:** The location where the focus region overlaps with the boundary. **E:** Masks are created of each cell. Each cell is a slightly different color, reflecting its (arbitrary) identity number. We can see that the indicated *P. aeruginosa* cell has four neighbors. **F:** Bordering pixels of the cell membrane. Different neighbors are indicated by different colors. Since it is not obvious from the summed image which boundary the focus is closest to, we look at the focus region instead. **G:** We can determine if the focus region on the boundary overlaps with *B. thailandensis* neighbors. Identification of foci localization toward *B. thailandensis* as identified in this manner is consistent with what we identified by eye.

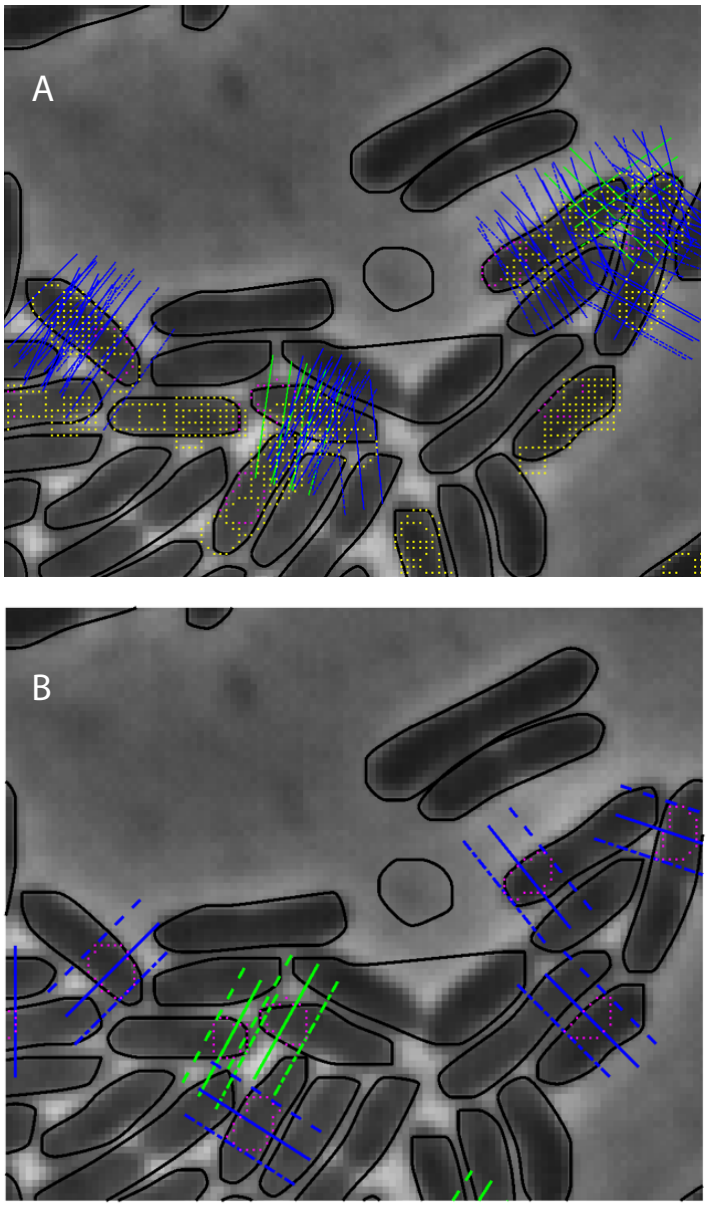

Figure 3.7: Demonstration of both simulation types. For each focus, three lines 100 nm long perpendicular to the nearest cell membrane were drawn at the edges and middle of the focus region. If lines from foci from different cells intersected, the lines were drawn as green. Else, drawn as blue. **Panel A:** For each cell with a focus, the focus was generated 10 times and determined if it matched with surrounding foci of cells. The foci of surrounding cells remained unchanged. Original foci are pink, generated foci are yellow. **Panel B:** For every cell with a focus, a new focus was generated. Then targeting was determined as normal. This was repeated 100 times. Foci in pink.

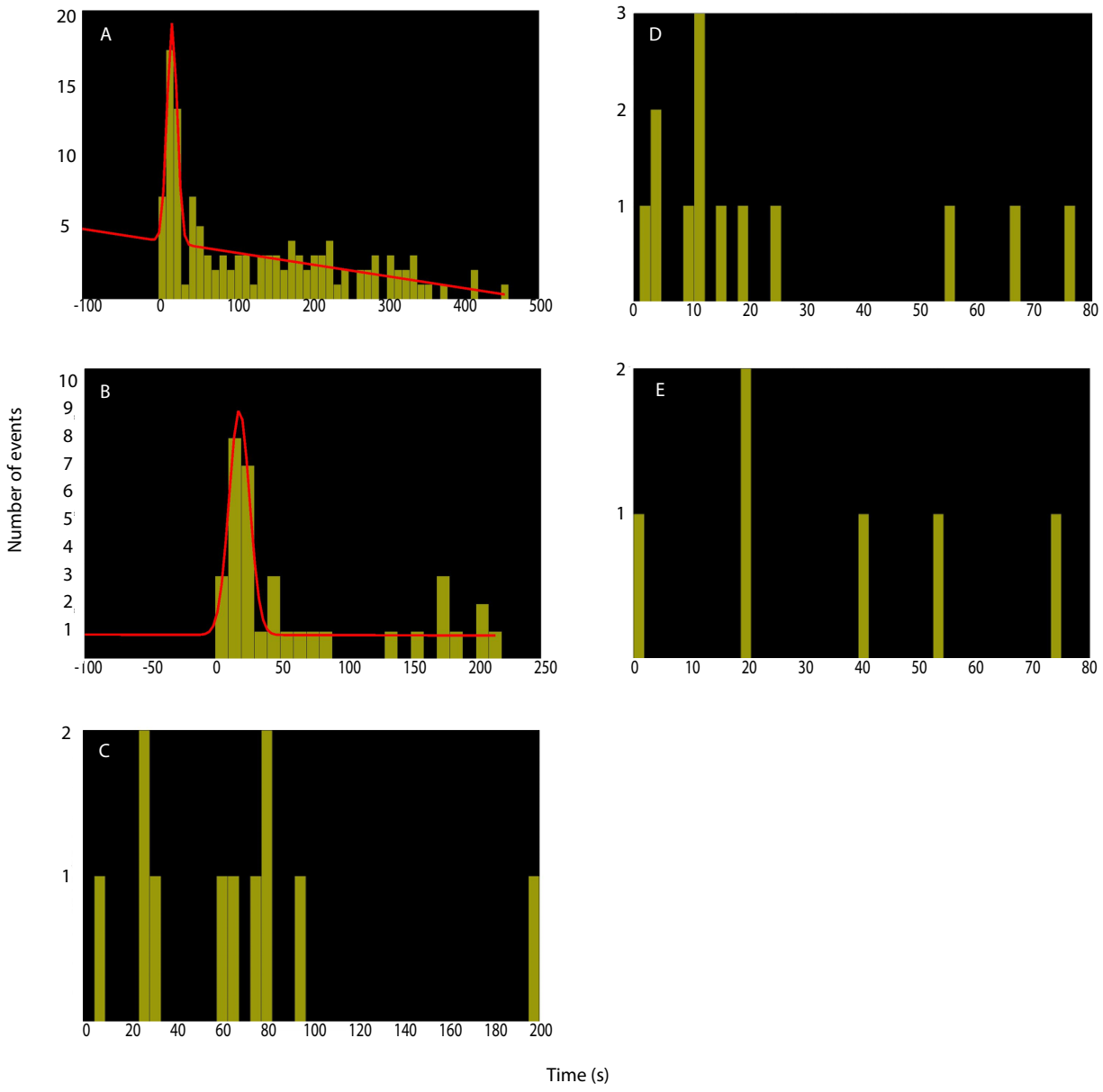

Figure 3.8: Response times between tit-for-tat behavior for different genetic strains. **A:** Δ*retS* response times over 9 minute timelapse. Fit in red is the sum of a line and a Gaussian function. The many long response times indicated that some of the identified tit-for-tat behavior was likely not due to a response, but due instead to frequent foci formation which happened to appear to match to previously formed foci. $n \approx 560$. **B:** To avoid confounding normal foci formation with foci forming in response to an attack, we investigated only foci where both foci appeared in the first four minutes of the time lapse. Fit in red is the sum of a line and a Gaussian function. Gaussian centered at 15 s. $n \approx 35$. Wild type, Δ*pppA* and Δ*tagF* strains all had significantly fewer events and a satisfactory fit was not able to be made. **C:** Wild type foci response times. $n \approx 80$. **D:** Δ*pppA* foci response times. $n \approx 145$. **E:** Δ*tagF* foci response times. $n \approx 60$.

Chapter 4

CONCLUSION AND FUTURE DIRECTIONS

4.1 Significance

Bacteria were once believed to be very simple organisms due to their microscopic size; they were in fact treated in my graduate level physics classes using the ”bag model”, approximating the inner workings of a bacterium as a bag with essential proteins diffusing randomly through the cytoplasm. However, bacteria have instead repeatedly surprised investigators with their complexity and ability to respond to their environment. The T6SS is one such example of bacterial complexity. Not only do these proteins assemble into a working apparatus rapidly in response to environmental signals, but the mechanisms used to deliver effectors to surrounding cells is beyond a simple hack of the genetically-related bacteriophage mechanism.

This work is particularly important as it relates to polymicrobial communities in clinical settings. *P. aeruginosa* is a particularly strong infection agent in lungs of cystic fibrosis patients, and implicated in 80% of cystic fibrosis deaths. While susceptible lungs are exposed to many different species of bacteria, *P. aeruginosa* is especially competent in this setting, frequently outcompeting many if not all other bacterial species and establishing itself in a biofilm. In this situation, it is exceptionally resistant to antibiotic treatment and is a significant contributor to health concerns of cystic fibrosis patients. Understanding interbacterial interactions of *P. aeruginosa* in general is widely recognized as useful toward addressing the *P. aeruginosa* infection. T6SS in *P. aeruginosa* in particular is important as it has strong antibacterial properties, and even more specifically H1-T6SS seems likely to be relevant in the cystic fibrosis setting. H1-T6SS is activated by growing on a surface (i.e. the interior of the lung) and sister cell lysate (often present in conditions with high cell

density and high exposure to antibacterial agents from antibiotics and/or surrounding bacteria of different species). Thus, it is to be expected that understanding interbacterial interactions based on T6SS will shed new light on the development of this infection in the lung.

This work both elucidates a new T6SS mechanism delivery model and suggests a more subtle approach to H1-T6SS targeting. While understanding T6SS activity is important to understand the progress of infection in clinical settings, my results in both these areas suggest that H1-T6SS is ideally situated to aid in bacterial competition under the clinical settings where the infection by *P. aeruginosa* is most often observed.

Beyond clinical relevance, this work suggests that homologous proteins in different species can maintain the same general function while serving a dramatically different role (i.e. ClpV, an ATPase, which in *V. cholerae* T6SS solely disassembles the TssBC sheath, but in *P. aeruginosa* provides the force generation for effector delivery). This diversity in mechanism, along with observations in other species which do not coincide perfectly with either the observations in *V. cholerae* or *P. aeruginosa*, suggests that several other mechanisms or variations on mechanism could be determined in other species possessing T6SSs. Additionally, these mechanisms appear to differ at least somewhat corresponding with activation conditions, with mechanisms set up to optimize cell killing under their specific activation conditions. Thus, studying effector delivery mechanisms is not important solely to understand the method of delivery but also to address the purpose behind each secretion system. This observation could explain why some bacterial species possess several copies of T6SS, as well as other antibacterial defense mechanisms such as T3SS; each is active under different and possibly non-overlapping conditions, and may have secretion mechanisms which match the respective activation conditions.

This work also raises interesting questions about targeting. While there are many studies demonstrating bacteria responding to their environment, there are very few studies showing antibacterial systems responding on a subcellular level to a threat. It is interesting to note that the $\Delta retS$ background shows subcellular targeting toward a threat,

while the wild type background does not have a noticeable level of targeting. It seems that targeting would add an advantage to H1-T6SS activity, especially since H1-T6SS is not constitutively active and responds to threats. Targeting on a subcellular level would, in theory, increase efficiency of H1-T6SS firing as far as cell killing. Thus, it is surprising that wild type does not also demonstrate the subcellular targeting observed so clearly in the Δ*retS* background. Δ*retS* derepresses T6SS gene expression via the Gac/Rsm pathway and promotes biofilm formation and H1-T6SS foci formation. It is possible that upregulating H1-T6SS via this pathway is representative of wild type behavior under nonstandard laboratory conditions. This hypothesis leads us to wonder how much of the observations about targeting are dependent on activation conditions, and if subcellular targeting is present in more antibacterial secretion systems but simply not triggered under standard laboratory conditions. This would have wide-ranging implications for interbacterial interaction study in many bacterial species.

4.2 Quantitative time-lapse fluorescence microscopy tools

At the population level, interbacterial interactions have primarily been studied using growth competition assays. However, this tool lacks the ability to resolve individual cells and clarify the importance of individual cell-cell interactions. I built off previous work from the Wiggins and Mougous labs to image bacteria with automated time-lapse fluorescence microscopy (TLFM) and computational tools to develop high-thoroughput, automated systems to characterize these individual cell behaviors. I adapted the pre-existing software from the Wiggins lab to track foci locations over time to identify foci repeating in the same location, wrote spike identification software, and created foci simulations to characterize observed behavior above random. Given these robust computational tools, we were able to analyze behavior which had never previously been measured in this context, including T6SS foci intensity over time, correlation functions between protein dynamics, and various simulations of foci behavior.

Before the work described in this thesis, it was an unstated assumption that the T6SS

secretion mechanism was conserved throughout all T6SSs. Additionally, the only study of T6SS mechanism was done in *V. cholerae*; despite several lines of evidence in other bacterial species where the *V. cholerae* syringe model did not seem to correspond with observed T6SS behavior, including different ratios of *S. marcescens* TssB and ClpV, no observations of TssB extending across the cell in any species, and repeated diffraction-limited foci in the same location in the cell in *S. marcescens*, other investigators did not see enough evidence to propose an entirely new model of effector delivery [22]. Especially given the several lines of evidence which lead us to propose this new model, and given the various conditions outlined in the introduction under which T6SS can be activated in different species, this is rather surprising; nature is known for using homologous proteins in unique ways in different species, and with these inconsistencies with the *V. cholerae* syringe model it is obvious that effector delivery must proceed in a different manner. This particularly makes sense in the context of activation of H1-T6SS; that this system tends to respond well when it is on a surface and when it senses sister cell lysate, meaning that it is most likely to be active under conditions where there is ideal biofilm conditions and high cell density (to achieve enough lysis events to generate enough lysate to sense). Therefore, in contrast to the rapid, one-shot *V. cholerae* T6SS, this system does not need to act rapidly, but can deliver the effectors to surrounding bacteria in a series of spiking events. My work demonstrated that the observed fluorescence microscopy differences in essential T6SS proteins are important and lead us to better understand the purpose of the H1-T6SS.

Additionally, I wrote tools to analyze the H1-T6SS targeting behavior on both cellular and a subcellular basis. Prior to my work, it was assumed that the tit-for-tat behavior observed in *P. aeruginosa* Δ*retS* background corresponded well to the behavior of wild-type H1-T6SS in *P. aeruginosa* [8]. However, in most previous studies (with the exception of [41]), all study of *P. aeruginosa* T6SS was done in the Δ*retS* background, and characterizations of tit-for-tat behavior lacked quantitative substance. I wrote my own software to correctly ascertain foci localization and targeting, correcting error-prone software from previous iterations of this analysis and quantitatively analyzing observed targeting in

comparison to simulations. This analysis suggests a different method of stimulus for H1-T6SS foci formation than has previously been hypothesized; in conjunction with the tit-for-tat behavior, previous studies had suggested that *P. aeruginosa* cells were more likely to form H1-T6SS foci near *P. aeruginosa* cells which also had H1-T6SS foci [40]. Since *P. aeruginosa* has immunity to its own T6SS toxins, and H1-T6SS is not active constitutively and it requires cell resources to create this system, this suggested that perhaps H1-T6SS was used as a signaling device between *P. aeruginosa* cells, encouraging neighbor *P. aeruginosa* cells to form their own lethal weapon since nearby cells had sensed a danger. My work clearly showed that this narrative is flawed, and that H1-T6SS is almost certainly not used as a signaling mechanism. Instead, the primary purpose of H1-T6SS is as originally thought before the incorrect studies, namely that it is used in interbacterial antagonism. It seems likely at this point that any above-random targeting of H1-T6SS toward a sister cell is responding to a general attack, not signaling to a sister cell to increase rate of H1-T6SS foci formation. To address further concerns, it is necessary to perform experiments with *B. thailandensis* T6SS foci labeled and mixed with all four genetic backgrounds described above and identify whether H1-T6SS localizes toward *B. thailandensis* T6SS foci at the same or a different rate as it localizes toward *P. aeruginosa* H1-T6SS foci. As the z-scores of the simulations are all quite high when comparing *P. aeruginosa* H1-T6SS foci localizing toward themselves, even though we know that two strains (Δ*pppA* and Δ*tagF*) cannot be targeting due to their localization restriction, it is important to compare the controls to the Δ*retS* and wild type strains, as done in Chapter 3 (see Table 3.1).

A limitation of the measurements is that the high intensity and frequency of fluorescent exposure ($\approx$every 2 seconds or every 5 seconds, depending on the experiment) required to resolve foci cannot be perpetuated for longer than $\approx$10-20 minutes due to bleaching and toxicity of exposure to fluorescence.

Another problem with the measurements I have taken is that we have assumed foci correspond with T6SS effector delivery. While it has been observed that increased number of foci correspond with increased T6SS-dependent cell killing ([35, 47]), it has so far

proved beyond our experimental capabilities to label T6SS effectors and observe their delivery from cell to cell. The only measurements done to show correlation between T6SS foci and cell killing are at a population level, not a cellular or subcellular level, and this ensemble average necessarily limits our understanding of protein function. Current data suggests that some H1-T6SS effectors require Hcp1 for stability, and localize to the inside of homohexameric Hcp rings. The *V. cholerae* syringe model suggests that these Hcp rings join to form tubules inside the TssBC sheath, and that the TssBC sheath contracts to push these Hcp rings into the exterior of the cell, thus delivering effectors to the location of the puncture caused by the Hcp tubule. In part for this reason, H1-T6SS effectiveness in *P. aeruginosa*, as in *V. cholerae* and other bacterial species possessing T6SSs, is often measured through Hcp secretion; this would indicate that secretion had occurred, rather than Hcp remaining in the cytoplasm. Since we propose a pump model rather than a syringe model for the *P. aeruginosa* H1-T6SS where several homologous proteins serve a similar but distinct purpose in effector delivery, it is also possible that effectors are not translocated through an Hcp tube, but rather another complex associated with Hcp. This mechanism could be elucidated through fluorescent labeling of one or more effectors or of Hcp, but as of time of this writing the fluorescent labels are too bulky to add to any of these key T6SS proteins, and the localization of these proteins, as well as the dynamic interactions with other key components of the H1-T6SS, is not known.

Previous work in the Wiggins lab, along with my own previously mentioned contributions, have established the method of study with two bacterial species in a monolayer, but polymicrobial communities are more commonly found with multiple organisms, and are also notably sensitive to specific environment conditions. Much of the reason for limiting the work to these specific conditions was due to the current quantification methodology of individual cells. Expanding our software to incorporate study of three-dimensional colonies and improved cell identification to allow more species to be tracked simultaneously would greatly aid our investigation in this field. Improved computational simulations addressing these complex situations would also advance this work. Future work

could investigate H1-T6SS behavior under environmental conditions more suited to clinically relevant scenarios, including multilayer colonies, permitted movement among cells, polymicrobial colonies including more than two species, and different growth media.

BIBLIOGRAPHY

[1]

[2] Sophie S. Abby, Jean Cury, Julien Guglielmini, Bertrand Neron, Marie Touchon, and Eduardo P.C. Rocha. Identification of protein secretion systems in bacterial genomes. *Scientific Reports*, 6(23080), 2016.

[3] M. S. Aschtgen, C. S. Bernard, Lloubs R. de Bentzmann, S., and E. Cascales. SciN is an outer membrane lipoprotein required for type VI secretion in enteroaggregative *Escherichia coli*.

[4] D. F. Aubert, R.S. Flannagan, and M.A. Valvano. A novel sensor kinase response regulator hybrid controls biofilm formation and type VI secretion system activity in *Burkholderia cenocepacia*. *Infectious Immunology*, 76:1979–1991, 2008.

[5] M. Barret, F. Egan, E. Fargier, J.P. Morrissey, and F. O'Gara. Genomic analysis of the type VI secretion systems in *Pseudomonas spp.*: novel clusters and putative effectors uncovered. *Microbiology*, 157.

[6] M. Basler and J. J. Mekalanos. Type 6 secretion dynamics within and between bacterial cells. *Science*, 337:815, 2012.

[7] M Basler, M Pilhofer, GP Henderson, GJ Jensen, and JJ Mekalanos. Type VI secretion requires a dynamic contractile phage tail-like structure. *Nature*, 483(7388):182–186, 2012.

[8] Marek Basler, Brian T Ho, and John J Mekalanos. Tit-for-tat: type VI secretion system counterattack during bacterial cell-cell interactions. *Cell*, 152(4):884–894, 2013.

[9] Christophe S. Bernard, Yannick R. Brunet, Erwan Gueguen, and Eric Cascales. Nooks and crannies in Type VI secretion regulation. *Journal of Bacteriology*, 192:3850–3860, 2010.

[10] Gabriele Bönemann, Aleksandra Pietrosiuk, Alexander Diemand, Hanswalter Zentgraf, and Axel Mogk. Remodelling of VipA/VipB tubules by ClpV-mediated threading is crucial for type VI protein secretion. *The EMBO journal*, 28(4):315–325, 2009.

[11] C. Bordi, M.C. Lamy, I. Ventre, E.Termine, A Hachani, S.Fillet, B. Roche, S. Sleves, V. Me jean, and other authors. Regulatory RNAs and the HptB/RetS signalling pathways fine-tune *Pseudomonas aeruginosa* pathogenesis. *Molecular Microbiology*, 76:1427–1443, 2010.

[12] Frédéric Boyer, Gwennaële Fichant, Jérémie Berthod, Yves Vandenbrouck, and Ina Attree. Dissecting the bacterial type VI secretion system by a genome wide in silico analysis: what can be learned from available microbial genomic resources? *BMC genomics*, 10(1):1, 2009.

[13] Yahua Chen, Jocelyn Wong, Guang Wen Sun, Yichun Liu, Gek-Yen Gladys Tan, and Yunn-Hwen Gan. Regulation of type VI secretion system during *Burkholderia pseudomallei* infection. *Infection and Immunity*, 79:3064–3073, 2011.

[14] S. Chugani and E.P. Greenberg. The influence of human respiratory epithelia on *Pseudomonas aeruginosa* gene expression. *Microbial Pathogenesis*, 42:29–35, 2007.

[15] Francesca R. Cianfanelli, Laura Monlezun, and Sarah J. Coulthurst. Aim, load, fire: The type VI secretion system, a bacterial nanoweapon. *Trends in Microbiology*, 24:51–62, April 2016.

[16] K.A. Coggan and M.C. Wolfgang. Global regulatory pathways and cross-talk control *Pseudomonas aeruginosa* environmental lifestyle and virulence phenotype. *Current Issues in Molecular Biology*, 14:47–70, 2012.

[17] Tiago R. D. Costa, Catarina Felisberto-Rodrigues, Amit Meir, Marie S. Prevost, Adam Redzej, Martina Trokter, and Gabriel Waksman. Secretion systems in Gram-negative bacteria colon structural and mechanistic insights. *Nature Reviews Microbiology*, 13:343–359, 2015.

[18] Q. Duan, M. Zhou, L. Zuh, and G. Zhu. Flagella and bacterial pathogenicity. *Journal of Basic Microbiology*, 53:1–8, 2013.

[19] J.P. Euzeby. List of bacterial names with standing in nomenclature: a folder available on the internet. *International Journal of System Bacteriology*, 47:590–592, 1997.

[20] Andreas Frster, Sara Planamente, Eleni Manoli, Nadine S. Lossi, Paul S. Freemont, and Alain Filloux. Coevolution of the ATPase ClpV, the sheath proteins TssB and TssC, and the accessory protein TagJ/HsiE1 distinguishes type VI secretion classes. *The Journal of Biological Chemistry*, 289(47):3303233043, 2014.

[21] M. Y. Galperin. A census of membrane-bound and intracellular signal transduction proteins in bacteria: bacterial IQ, extroverts and introverts. *Biomedical Central Microbiology*, 5.

[22] Amy J. Gerc, Andreas Diepold, Katharina Trunk, Michael Porter, Colin Rickman, Judith P. Armitage, Nicola R. Stanley-Wall, and Sarah J. Coulthurst. Visualization of the *Serratia* type VI secretion system reveals unprovoked attacks and dynamic assembly. *Cell Reports*, 12(12):2131 – 2142, 2015.

[23] R.G. Gerlach and M. Hensel. Protein secretion systems and adhesins: the molecular armory of Gram-negative pathogens. *International Journal of Medical Microbiology*, 297:401–415, 2007.

[24] A.L. Goodman, B. Kulasekara, A. Rietsch, D. Boyd, R.S. Smith, and S. Lory. A signaling network reciprocally regulates genes associated with acute infection and chronic persistence in *Pseudomonas aeruginosa*. *Developmental Cell*, 7:745–754, 2004.

[25] Phyllis I Hanson and Sidney W Whiteheart. AAA+ proteins: have engine, will work. *Nature Reviews Molecular Cell Biology*, 6(7):519–529, 2005.

[26] K.A. Hassan, A. Johnson, B.T. Shaffer, Q. Ren, T.A. Kidarsa, L. D. Elbourne, S. Hartney, R. Duboy, and N. C. Goebel. Inactivation of the GacA response regulator in *Pseudomonas fluorescens* Pf-5 has far-reaching transcriptomic consequences.

[27] Christopher S. Hayes, Stephanie K. Aoki, and David A. Low. Bacterial contact-dependent delivery systems. *Bioessays*, 44:71–90, September 2010.

[28] D. M. Heithoff, W. R. Shimp, J. K. House, Y. Xie, B.C. Weimer, and R. L. Sinsheimer. Intraspecies variation in the emergence of hyperinfectious bacterial strains in nature. *PLoS Pathology*, 8, 2012.

[29] Brian T. Ho, Marek Basler, and John J. Mekalanos. Type 6 secretion system-mediated immunity to type 4 secretion system-mediated gene transfer. *Science*, 342:250–253, 2013.

[30] Rachel D. Hood, Pragya Singh, FoSheng Hsu, Tzn Gvener, Mike A. Carl, Rex R.S. Trinidad, Julie M. Silverman, Brooks B. Ohlson, Kevin G. Hicks, Rachael L. Plemel, Mo Li, Sandra Schwarz, Wenzhuo Y. Wang, Alexey J. Merz, David R. Goodlett, and Joseph D. Mougous. A type VI secretion system of *Pseudomonas aeruginosa* targets a toxin to bacteria. *Cell Host Microbe*, 7:25–37, 2010.

[31] FoSheng Hsu, Sandra Schwarz, and Joseph D Mougous. TagR promotes PpkA-catalysed type VI secretion activation in *Pseudomonas aeruginosa*. *Molecular microbiology*, 72(5):1111–1125, 2009.

[32] Bo Huang, Hazen Babcock, and Xiaowei Zhuang. Breaking the diffraction barrier: super-resolution imaging of cells. *Cell*, 143(7):1047–58, dec 2010.

[33] Cristoph J Hueck. Type III protein secretion systems in bacterial pathogens of animals and plants. *Microbiology and Molecular Biology Reviews*, 62, 1998.

[34] T Ishikawa, PK Rompikuntal, B Lindmark, DL Milton, and SN Wai. Quorum sensing regulation of the two Hcp alleles in *Vibrio cholerae* O1 strains. *PLoS One*, 4, 2009.

[35] Nicole Kapitein, Gabriele Bönemann, Aleksandra Pietrosiuk, Fabian Seyffer, Ingrid Hausser, Jacomine Krijnse Locker, and Axel Mogk. ClpV recycles VipA/VipB tubules and prevents non-productive tubule formation to ensure efficient type VI protein secretion. *Molecular microbiology*, 87(5):1013–1028, 2013.

[36] Anna Konovalova and Lotte Sgaard-Andersen. Close encounters: contact-dependent interactions in bacteria. *Molecular Microbiology*, 81:297–301, July 2011.

[37] Nathan J Kuwada, Keith C Cheveralls, Beth Traxler, and Paul A Wiggins. Mapping the driving forces of chromosome structure and segregation in *Escherichia coli*. *Nucleic acids research*, page 468, 2013.

[38] D. Lalaouna, S. Fochesato, L. Sanchez, P. Schmitt-Kopplin, D. Haas, T. Heulin, and W. Achouak. Phenotypic switching in *Pseudomonas brassicacearum* involves GacS- and GacA-dependent Rsm small RNAs. *Applied Environmental Microbiology*, 78:1658–1665.

[39] Karine Lapouge, Mario Schubert, Frédéric H-T Allain, and Dieter Haas. Gac/Rsm signal transduction pathway of γ-proteobacteria: from RNA recognition to regulation of social behaviour. *Molecular microbiology*, 67(2):241–253, 2008.

[40] Michele LeRoux, Justin A. De Leon, Nathan J. Kuwada, Alistair B. Russell, Delia Pinto-Santini, Rachel D. Hood, Danielle M. Agnello, Stephen M. Robertson, Paul A. Wiggins, and Joseph D. Mougous. Quantitative single-cell characterization of bacterial interactions reveals type VI secretion is a double-edged sword. *Proceedings of the National Academy of Sciences*, 109(48):19804–19809, 2012.

[41] Michele LeRoux, Robin L Kirkpatrick, Elena I Montauti, Bao Q Tran, S Brook Peterson, Brittany N Harding, John C Whitney, Alistair B Russell, Beth Traxler, Young Ah

Goo, David R Goodlett, Paul A Wiggins, and Joseph D Mougous. Kin cell lysis is a danger signal that activates antibacterial pathways of *Pseudomonas aeruginosa*. *eLife*, page e05701, 2015.

[42] B Lesic, M Starkey, J He, R Hazan, and LG Rahme. Quorum sensing differentially regulates *Pseudomonas aeruginosa* type VI secretion locus I and homologous loci II and III, which are required for pathogenesis. *Microbiology*, 155:2845–2855, 2009.

[43] Jer-Sheng Lin, Hsin-Hui Wu, Pang-Hung Hsu, Lay-Sun Ma, Yin-Yuin Pang, Ming-Daw Tsai, and Erh-Min Lai. Fha interaction with phosphothreonine of TssL activates type VI secretion in *Agrobacterium tumefaciens*. *PLoS Pathog*, 10(3):e1003991, 2014.

[44] Nadine Lossi, Eleni Manoli, Pete Simpson, Cerith Jones, Kailyn Hui, Rana Dajani, Sarah J Coulthourst, Paul Freemont, and Alain Filloux. The archetype *Pseudomonas aeruginosa* proteins TssB and TagJ form a novel subcomplex in the bacterial type VI secretion system. *Molecular microbiology*, 86(2):437–56, 2012.

[45] Sarah T. Miyata, Verena Bachmann, and Stefan Pukatzki. Type VI secretion system regulation as a consequence of evolutionary pressure. *Journal of Medical Microbiology*, 62:663–676, 2013.

[46] Joseph D. Mougous, Marianne E. Cuff, Stefan Raunser, Aimee Shen, Min Zhou, Casey A. Gifford, Andrew L. Goodman, Grazyna Joachimiak, Claudia L. Ordoñez, Stephen Lory, Thomas Walz, Andrzej Joachimiak, and John J. Mekalanos. A virulence locus of *Pseudomonas aeruginosa* encodes a protein secretion apparatus. *Science*, 312(5779):1526–1530, 2006.

[47] Joseph D Mougous, Casey A Gifford, Talia L Ramsdell, and John J Mekalanos. Threonine phosphorylation post-translationally regulates protein secretion in *Pseudomonas aeruginosa*. *Nature cell biology*, 9(7):797–803, 2007.

[48] H.E. O'Brien, D. Desveaus, and D.S. Guttman. Next generation genomics of *Pseudomonas syringae*. *Current Opinion in Microbiology*, 14:24–30, 2011.

[49] N. J. Palleroni. *Introduction to the Pseudomonadaceae.* Springer, 1992.

[50] Rob Phillips, Jane. Kondev, and Julie. Theriot. *Physical biology of the cell*. Garland Science, 2009.

[51] Aleksandra Pietrosiuk, Esther D. Lenherr, Sebastian Falk, Gabriele Bnemann, Jrgen Kopp, Hanswalter Zentgraf, Irmgard Sinning, and Axel Mogk. Molecular basis for the unique role of the AAA+ chaperone ClpV in type VI protein secretion. *Journal of Biological Chemistry*, 286, 2011.

[52] S. L. Porter, G. H. Wadhams, and J. P. Armitage. Signal processing in complex chemotaxis pathways. *Nature Review Microbiology*, 9:153–65, 2011.

[53] E. Potvin, D.E. Lehoux, I. Kukavica-Ibrulj, K.L. Richard, F. Sanschagrin, G.W. Lau, and R.C. Levesque. In vivo functional genomics of *Pseudomonas aeruginosa* for high-throughput screening of new virulence factors and antibacterial targets. *Environmental Microbiology*, 5:1294–1308, 2003.

[54] Dmitry Ratner, M. Pontus A. Orning, and Egil Lien. Bacterial secretion systems and regulation of inflammasome activation. *Journal of Leukocyte Biology*, 101(1):165–181, 2016.

[55] A.R. Records and D.C. Gross. Sensor kinases RetS and LadS regulate *Pseudomonas syringae* type VI secretion and virulence factors. *Journal of Bacteriology*.

[56] AB Russell. Type VI secretion delivers bacteriolytic effectors to target cells. *Nature*, 475:343–347, 2011.

[57] Alistair B. Russell, S. Brook Peterson, and Joseph D. Mougous. Type VI secretion system effectors: poisons with a purpose. *Nature Reviews Microbiology*, 12:137–148, 2014.

[58] P.F. Sarris and E.V. Scoulica. *Pseudomonas entomophila* and *Pseudomonas endocina*: potential models for studying the bacterial type VI secretion system. *Infection, Genetics and Evolution*, 11:1352–1360, 2011.

[59] M. A. Schell, R.L. Ulrich, J.W. Ribot, E.E. Brueggemann, H.B. Hines, D. Chen, L. Lipscomb, H.S. Kim, and J. Mrazek. Type VI secretion is a major virulence determinant in *Burkholderia mallei*. *Molecular Microbiology*, 64:1466–1485, 2007.

[60] Christian Schlieker, Hanswalter Zentgraf, Petra Dersch, and Axel Mogk. ClpV, a unique Hsp100/Clp member of pathogenic proteobacteria. *Biological chemistry*, 386(11):1115–1127, 2005.

[61] S. Schwarz, T.E. West, F. Boyer, W.C. Chiang, M. A. Carl, R.D. Hood, L. Rohmer, T. Tolker-Nielsen, S.J. Skerrett, and J.D. Mougous. *Burkholderia* type VI secretion systems have distinct roles in eukaryotic and bacterial cell interactions. *PLoS Pathology*, 6(e1001068), 2010.

[62] Osamu Shimomura, Frank H. Johnson, and Yo Saiga. Extraction, Purification and Properties of Aequorin, a Bioluminescent Protein from the Luminous Hydromedusan, Aequorea. *Journal of Cellular and Comparative Physiology*, 59(3):223–239, jun 1962.

[63] M.W. Silby, C. Winstanley, S.A. Godfrey, S.B.Levy, and R.W. Jackson. *Pseudomonas* genomes: diverse and adaptable.

[64] Julie M Silverman, Laura S Austin, FoSheng Hsu, Kevin G Hicks, Rachel D Hood, and Joseph D Mougous. Separate inputs modulate phosphorylation-dependent and-independent type VI secretion activation. *Molecular microbiology*, 82(5):1277–1290, 2011.

[65] C.J. Southey-Pillig, D.G. Davies, and K. Sauer. Characterization of temporal protein production in *Pseudomonas aeruginosa* biofilms. *Journal of Bacteriology*, 187:8114–8126, 2005.

[66] M. Starkey and L.G. Rahme. Modeling *Pseudomonas aeruginosa* pathogenesis in plant hosts. *Nature Protocols*, 4:117–124, 2009.

[67] C. K. Stover, X. Q. Pham, A. L. Erwin, S. D. Mizoguchi, P. Warrener, M. J. Hickey, F.S. L. Brinkman, W. O. Hufnagle, D. J. Kowalik, M. Lagrou, R. L. Garber, L. Goltry, E. Tolentino, S. Westbrock-Wadman, Y. Yuan, L. L. Brody, S. N. Coulter, K. R. Folger, A. Kas, K. Larbig, R. Lim, K. Smith, D. Spencer, G. K.-S. Wong, Z. Wu, I. T. Paulsen, J. Reizer, M. H. Saier, R. E. W. Hancock, S. Lory, and M. V. Olson. Complete genome sequence of *Pseudomonas aeruginosa* PAO1, an opportunistic pathogen. *Nature*, 406:959–64, 2000.

[68] Reed M. Stubbendieck, Carol Vargas-Bautista, and Paul D. Straight. Bacterial communities: Interactions to scale. *Frontiers in Microbiology*, 7(1234), 2016.

[69] Stella Stylianidou, Connor Brennan, Silas B. Nissen, Nathan J. Kuwada, and Paul A. Wiggins. SuperSegger: robust image segmentation, analysis and lineage tracking of bacterial cells. *Molecular Microbiology*, 102(4):690–700, 2016.

[70] I. Ventre, A.L. Goodman, I. Vallet-Gely, P. Vassseur, C. Soscia, S. Molin, S. Sleves, A. Lazdunski, S. Lory, and A. Filloux. Multiple sensors control reciprocal expression of *Pseudomonas aeruginosa* regulatory RNA and virulence genes.

[71] Isabelle Ventre, Andrew L. Goodman, Isabelle Vallet Gely, Perrine Vasseur, , Chantal Soscia, Soren Molin, Sophie Bleves, Andree Lazdunski, Stephen Lory, and Alain Filloux. Multiple sensors control reciprocal expression of *Pseudomonas aeruginosa* regulatory RNA and virulence genes. *PNAS*, 103(1):171–176, 2005.

[72] Andrea Vettiger and Marek Basler. Type VI secretion system substrates are transferred and reused among sister cells. *Cell*, 167:99–110, 2016.

[73] P. Williams. Quorum sensing, communications, and cross-kingdom signaling in the bacterial world. *Microbiology*, 153:3923–38, 2007.

[74] Yiting Yu, H. Stanley Kim, Hui Hoon Chua, Chi Ho Lin, Siew Hoon Sim, Daoxun Lin, Alan Derr, Reinhard Engels, David DeShazer, Bruce Birren, William C. Nierman, and Patrick Tan. Genomic patterns of pathogen evolution revealed by comparison of *Burkholderia pseudomallei*, the causative agent of melioidosis, to avirulent *Burkholderia thailandensis*. *BMC Microbiology*, 6(1):46, 2006.